Title
FURTHER CONSIDERATIONS ON THE INCONSISTANCY IN TOUGHNESS EVALUATION OF ULTRA-HIGH STRENGTH STEEL AUSTENITIZED AT INCREASING TEMPERATURES

Author
Ritchie, R.O.

Publication Date
1977-07-01

Submitted to Metallurgical
Transactions A

LBL-6606 c./
Preprint

FURTHER CONSIDERATIONS ON THE INCONSISTANCY IN TOUGHNESS EVALUATION OF ULTRA-HIGH STRENGTH STEEL AUSTENITIZED AT INCREASING TEMPERATURES

Robert O. Ritchie and R. M. Horn

July 1977

Prepared for the U. S. Energy Research and
Development Administration under Contract W-7405-ENG-48

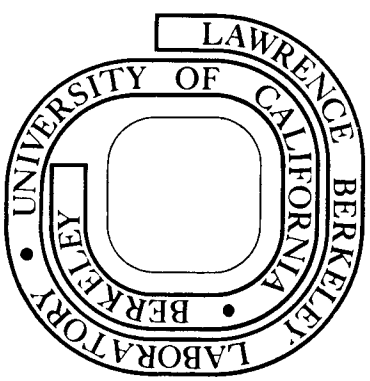

DISCLAIMER

Submitted to Metallurgical Transactions A LBL-6606

FURTHER CONSIDERATIONS ON THE INCONSISTANCY IN TOUGHNESS EVALUATION OF ULTRA-HIGH STRENGTH STEEL AUSTENITIZED AT INCREASING TEMPERATURES

Robert O. Ritchie and R. M. Horn

Materials and Molecular Research Division, Lawrence Berkeley Laboratory
and Department of Materials Science and Mineral Engineering,
University of California, Berkeley, California 94720

July 1977

Robert O. Ritchie is Assistant Professor, Department of Mechanical Engineering, Massachusetts Institute of Technology, Cambridge MA 02139, formally with the Lawrence Berkeley Laboratory, University of California in Berkeley. R. M. Horn is Associate Development Engineer, Department of Materials Science and Mineral Engineering, University of California, Berkeley, CA 94720.

ABSTRACT

A study has been made of the influence of austenitizing temperature on the ambient temperature toughness of commercial AISI 4340 ultra-high strength steel in the as-quenched (untempered) and quenched and tempered at 200°C conditions. As suggested in previous work, a systematic trend of *increasing* plane strain fracture toughness (K_{Ic}) and *decreasing* Charpy V-notch energy is observed as the austenitizing temperature is raised while the yield strength remains unaffected. This effect is seen under both static (slow-bend) and dynamic (impact) loading conditions, and is rationalized in terms of a differing response of the microstructure, produced by each austenitizing treatment, to the influence of notch root radius on toughness. Since failure in all microstructures was observed to procede primarily by a ductile rupture (microvoid coalescence) mechanism, an analysis is presented to explain these results, similar to that reported previously for stress-controlled fracture, based on the assumption that ductile rupture can be considered to be strain-controlled. Under such conditions, the decrease in V-notch Charpy energy is associated with a reduction in critical fracture strain at increasing austenitizing temperatures, consistent with an observed decrease in uniaxial and plane strain ductility. The increase in sharp-crack fracture toughness, on the other hand, is associated with an increase in "characteristic distance" for ductile fracture, resulting from dissolution of void-initiating particles at high austenitizing temperatures. The microstructural factors which

affect this behavior are discussed, and in particular the specific role of retained austenite is examined. No evidence was found that the enhancement of fracture toughness at high austenitizing temperatures was due to the presence of films of retained austenite. The significance of this work on commonly-used Charpy/K_{Ic} empirical correlations is briefly discussed.

INTRODUCTION

Commercial ultra-high strength, low alloy steels, such as the AISI 43XX series, are conventionally austenitized at low temperatures (typically 870°C) before quenching and tempering to produce fine prior austenite grain sizes, insuring good combinations of strength and impact toughness.[1] Recently, however, there has been considerable interest in employing much higher austenitizing temperatures (up to 1200°C) to increase the fracture toughness, K_{Ic}, of such steels without loss in strength.[1-8] Unfortunately, although increases in fracture toughness by over a factor of two have been reported following such high temperature austenitizing treatments, this marked improvement in K_{Ic} is often not paralleled with a corresponding increase in Charpy V-notch impact energy.[6,9-14] In fact a *decrease* in Charpy energy has been observed concurrent with the *increase* in K_{Ic} for Ni-Cr-Mo,[9] Ni-Cr-Mo-V[9] and Fe-Cr-C[13] steels, En25,[11] 4340,[4,10,12,14] and 300-M[4] steels, in both as-quenched and quenched and tempered (< 350°C) conditions. An explanation for this apparent paradox,[10] where structures resulting from high temperature austenitization show the largest toughness when rated by K_{Ic} and structures conventionally austenitized at low temperatures show the largest toughness when rated by Charpy energy, has been proposed by Ritchie et al.[10] in terms of the basic differences between the plane strain fracture toughness (K_{Ic}) test and the Charpy V-notch impact test. It was shown that the observed behavior was independent of shear lip energy and strain rate

effects, and could be rationalized in terms of the differing response of the structure produced by each austenitizing treatment to the influence of notch root radius (ρ) on toughness.* By considering only stress-controlled fracture mechanisms, ie. quasi-cleavage and intergranular fracture, where the critical fracture event can be considered to occur when the maximum principal stress (σ_{yy}) at the notch tip exceeds the fracture stress (σ_F), Ritchie et al.[10] argued that for failure ahead of a sharp crack (ie. a fatigue pre-crack in a K_{Ic} specimen) σ_{yy} must exceed σ_F over a certain "characteristic" distance[16] (ℓ), representing the microstructurally significant extent of the process zone ahead of the notch tip. Ahead of a sharp crack where the maximum tensile stress (σ_{yy}^{max}) is in close proximity to the notch, this distance characterizes the minimum distance from the tip where the critical fracture event can occur (ie. $\sigma_{yy} > \sigma_F$). By increasing the austenitizing temperature, the resultant coarsening of the microstructure gives rise to an increase in characteristic distance which leads to an increase in fracture toughness, K_{Ic}. Ahead of a blunt notch, however, as in the case of the Charpy V-notch specimen where $\rho \approx 0.25$ mm, the maximum tensile stress is located close to the elastic-plastic interface well beyond the characteristic distance. In this situation the toughness is controlled by the fracture stress (σ_F), with an increased austenitizing temperature leading to a

*Floreen[15] arrived at a similar conclusion in explaining conflicting K_{Ic} and Charpy impact toughness results observed in a study of fracture behavior of cast and wrought high strength 4340, stainless and maraging steels.

decrease in σ_F and to a resulting decrease in toughness. A schematic representation of these fracture events, reproduced from Ref. 10, is shown in Fig. 1.

It is important to note that the above analysis is only strictly valid for stress-controlled fracture mechanisms, as shown, for example, by as-quenched, untempered AISI 4340 after austenitizing at 870°C and at 1200°C followed by a step-quench at 870°C. When 4340 is direct oil quenched from intermediate austenitizing temperatures and/or tempered at 200°C (the commercially-used tempering temperature), the resulting failure mechanisms are primarily by ductile rupture (microvoid coalescence). Attempts[17,18] to apply the above analysis to such ductile fractures have, not surprisingly, met with little success, since microvoid coalescence cannot be described in terms of a stress-controlled fracture process. The object of the present investigation is to modify the previous analysis,[10] for ductile fracture, using a strain-controlled fracture criterion, to explain the observed fracture behavior of a purer heat of 4340 in untempered and tempered at 200°C conditions (following direct oil quenching) over the entire range of austenitizing temperature from 870°C to 1200°C. Furthermore, in the light of the somewhat conflicting claims[2-4,6,7,19-21] for the microstructural origin of the effect of austenitizing treatment on toughness, an attempt is made to examine the specific role of retained austenite, which has been widely attributed[1,46,19-21] as the source of improved fracture toughness in high temperature austenitized steels.

EXPERIMENTAL PROCEDURE

The material used in the investigation was aircraft-quality (vacuum-arc remelted) AISI 4340 hot-rolled bar, received in the fully annealed condition, and having the following composition (wt pct):

C	Mn	Cr	Ni	Mo	Si	S	P	Cu
0.41	0.80	0.79	1.75	0.23	0.23	0.004	0.006	0.06

This composition was chosen to represent a purer heat of the 4340 steel which was utilized in previous investigations of Lai et al.[6] and Ritchie et al.[10]

As-received material was hot forged and hot rolled to desired thicknesses, and subsequently slow cooled and spheroidized at 650°C for 1h to insure good machinability. Test specimens were heat-treated by austenitizing for 1h at temperatures of 870°C, 1000°C, 1100°C and 1200°C prior to being direct quenched into agitated oil, yielding a variation in prior austenite grain size from 20 to 230 μm (Fig. 2). The majority of specimens were tested in the as-quenched, untempered condition. To provide a comparison with commercially-used treatments, however, a further series of specimens was austenitized and oil quenched as above, and then tempered for 1h at 200°C. Toughness properties were determined at ambient temperature (22°C) under both "static" (rate of increase in stress intensity at notch tip, $\dot{K} \lesssim 3$ MPa$\sqrt{m}$/s) and "dynamic" ($\dot{K} \sim 10^5$-10^6 MPa$\sqrt{m}$/s) conditions.

For fracture ahead of sharp notches (ie. fatigue pre-cracks where the notch root radius $\rho \rightarrow 0$), "static" plane strain fracture toughness tests to measure K_{Ic} were performed on 25.4 mm thick 1-T compact tension specimens in accordance with ASTM specifications.[22] All K_{Ic} values were found to be "valid" with respect to this specification. Dynamic fracture toughness (K_{Id}) values were determined using fatigue pre-cracked standard Charpy specimens broken using an instrumented Charpy impact machine at a hammer velocity of 1.36 m/s. For fracture ahead of rounded notches, tests were conducted on standard sized (10 mm sq) ASTM Charpy V-notch specimens[23] (where $\rho \approx 0.25$ mm), both under 3-point slow-bend conditions (for static values) and in a pendulum type impact machine with a hammer velocity of 3.3 m/s (for dynamic values). A further series of tests was performed using Charpy V-notch specimens, tested in 3-point slow bend, where the notch root radius ρ was varied from 0.025 to 0.40 mm, to assess the influence of root radius on static toughness. All test-pieces were machined in the longitudinal (L-T) orientation.

Ambient temperature uniaxial tensile properties were determined both with 25.4 mm gage length cylindrical tensile bars, tested under displacement control on an electro servo-hydraulic M.T.S. testing machine, and with 25.4 mm gage length flat tensile bars, tested on an Instron Universial (screw-driven) testing machine, at a displacement rate of 0.5 mm/min. Yield and tensile strength measurements were averaged from both tests, whereas uniaxial ductility measurements (percentage elongation and reduction in area) were only calculated

from the cylindrical tensile specimens. To provide a better measurement of the ductility of material close to the notch tip in fracture specimens, an assessment was made of plane strain ductility values, determined using plane strain tension test-pieces of the design shown in Fig. 3. Details of the procedure for measuring plane strain ductility with such specimens has been described elsewhere.[24]

Magnetic saturation induction measurements, using a permeameter,[25] were performed during monotomic tensile tests of the flat tensile specimens to assess the extent of any deformation-induced austenite-to-martensite transformation. Initial (un-deformed) levels of retained austenite in the structures were checked using standard X-ray techniques.[26] Microstructure and fracture morphology were characterized using optical, transmission and scanning electron microscopy.

RESULTS

1. Uniaxial Tensile Properties

The influence of austenitizing temperature on ambient temperature, uniaxial, tensile properties of AISI 4340 steel is shown in Figs. 4 and 5 for as-quenched material and material tempered at 200°C respectively. As reported previously[10] yield and tensile strengths of the steel are largely unaffected by an increase in austenitizing temperature, although a marginal reduction in yield strength may be noted for tempered structures. The true stress at fracture, measured from the failure load in a tensile test, can be seen to decrease as the solution temperature is raised.

2. Toughness Evaluation

Despite the insignificant change in strength, there are large variations in toughness as austenitizing temperature is raised, as shown in Figs. 6 to 9 for AISI 4340. Plotted in Fig. 6 are, what one may term, "sharp-crack" toughness values, representing toughness values measured in specimens containing sharp (ie. fatigue pre-cracked, $\rho \sim 0$) cracks. In this instance, static and dynamic fracture toughness values (K_{Ic} and K_{Id} respectively) are plotted as a function of austenitizing temperature. Figure 7 shows the variation of "rounded-notch" toughness with austenitizing temperature, representing toughness values measured in specimens containing blunt (V-notched, $\rho \approx 0.25$ mm) notches. Here Charpy V-notch absorbed energy is plotted both for static (slow-bend) and dynamic (impact) loading conditions.

Also shown is an assessment of toughness computed from the area under uniaxial tensile stress-strain curves in test-pieces containing no notches. These plots indicate a consistent trend of *increasing* K_{Ic}, yet *decreasing* Charpy V-notch energy with increase in austenitizing temperature. Irrespective of the strain rate (or $\dot{K}$) of testing, the toughness evaluated in sharp-cracked specimens (K_{Ic}, K_{Id}) is seen to be increased,* with increasing austenitizing temperature, whereas the toughness evaluated in rounded-notched specimens (slow-bend and impact Charpy V-notch energy) is seen to be decreased. Similar trends are apparent for 4340 steel after tempering at 200°C, as illustrated in Figs. 8 and 9. For such tempered structures, the increase in K_{Ic} after high temperature austenitization is particularly significant, rising from K_{Ic} = 56 MPa$\sqrt{m}$ after direct quenching from 870°C to K_{Ic} = 92 MPa$\sqrt{m}$ after direct quenching from 1200°C (Fig. 8).

As observed previously,[10] mechanisms of fracture for a given structure were found independent of strain rate and independent of the technique used to assess toughness. Scanning electron fractographs for both as-quenched and quenched and tempered 4340 are shown in Figs. 10 and 11, where it can be seen that failure occurred by a ductile rupture mechanism (microvoid coalescence) for all structures, with the exception of the structure as-quenched from 870°C (Fig. 10a) which shows additional evidence of intergranular and quasi-cleavage

*K_{Ic} and K_{Id} values are lowered somewhat above 1100°C in direct as-quenched structures. This result is not observed for step-quenched structures,[14] nor after tempering (Fig. 8), and is unexplained at this time.

fracture. The size and spacing of dimples involved in the particle-induced fracture can, however, be seen to have increased as the austenitizing temperature was raised. This is clearly demonstrated in Fig. 11 for tempered structures.

3. Variation of Toughness with Notch Root Radius

As concluded in the previous study,[10] the contradictory toughness results measured on K_{Ic} and Charpy V-notch test-pieces with increase in austenitizing temperature cannot be accounted for by change in loading rate, since similar behavior is seen under both static and dynamic conditions. Again it appears that the dimensions of the notch root radius are of paramount importance in determining whether "toughness" increases or decreases as the austenitizing temperature is raised. To examine this further, a series of Charpy V-notch specimens were tested in 3-point bend under static (slow bend) loading conditions, with the radius of the notch varied from $\rho \sim 0$ (ie. fatigue pre-cracked) to $\rho \approx 320$ μm. Results are illustrated in Fig. 12 for as-quenched 4340 in the form of plots of "apparent" fracture toughness $(K_A)^*$ versus the square root of the notch radius $(\rho^{1/2})$. The toughness behavior observed (Fig. 12) is very similar to that reported for stress-controlled fracture in 4340,[10] in that at small root radii ($\rho \lesssim 25$ μm), toughness increases with austenitizing temperature (up to 1100°C), whereas at large root radii, toughness decreases.

*"Apparent" fracture toughness (K_A) here refers to the value of K_{Ic} measured ahead of a notch of root radius ρ, and is a parameter commonly used to estimate fracture toughness without resource to fatigue pre-cracking.[10,12,27-29]

However, for the present results, fracture primarily occurs by non-stress controlled fracture mechanisms, namely ductile rupture, and thus the previous model[10] to explain such results is not applicable. Accordingly, an alternative approach is now presented for failure by ductile rupture, based on the assumption that this fracture mechanism can be considered to be strain-controlled.

4. Model for Influence of Notch Root Radius on Toughness Evaluation

In the previous investigation,[10] where contradictory toughness results (similar to those shown in Fig. 12) were observed in as-quenched 4340 for fracture by quasi-cleavage and intergranular cracking, an interpretation was presented based on a simple model,[27,28] for stress-controlled fracture, of the influence of notch root radius (ρ) on toughness. Under elastic-perfectly plastic conditions, where failure is taken to occur when the maximum tensile stress ahead of the notch tip exceeds a critical fracture stress (σ_F), the variation in toughness with ρ can be described by

$$K_A \approx 2.9\ \sigma_y [\exp(\sigma_F/\sigma_y - 1) - 1]^{1/2}\ \rho^{1/2} \quad , \qquad (1)$$

where σ_y is the yield stress and K_A the apparent fracture toughness. In this instance, the slope of the K_A vs. $\rho^{1/2}$ plot (eg. Fig. 12) can be related to the critical fracture stress (σ_F). Since this slope decreases with increase in austenitizing temperature, the reduction in V-notch toughness with increasing austenitizing temperature was associated with a decrease in σ_F for stress-controlled fracture.

In the present case, the same trends are evident (Fig. 12) even though fracture is occurring by ductile rupture. Thus, by assuming the failure mechanism of ductile rupture to be primarily strain-controlled, we may proceed to re-examine this effect of notch radius on toughness.

Following Rice,[30] we consider a flat surface notch with a smooth tip radius ρ. By examining the strain concentration at the tip under plane strain conditions, it can be shown[30] that the extensional strain (ε) at the notch surface, directly ahead of the tip, is given by

$$\varepsilon = \frac{3}{4}\left(\varepsilon_y + \frac{J}{\sigma_y \rho}\right) \quad , \tag{2a}$$

where

$$\varepsilon_y = (1-\nu^2)\ \sigma_y/E \quad , \tag{2b}$$

and

$$J = (1-\nu^2)\ K^2/E \quad . \tag{2c}$$

ε_y is the yield strain, σ_y the yield stress, J the path independent J-integral, K the apparent stress intensity ahead of notch, radius ρ, ν Poisson's ratio, and E the Elastic modulus. By rearranging terms, the apparent stress intensity K is given by

$$K^2 = \left[\frac{4}{3(1-\nu^2)}\right]\ \sigma_y\ \rho E(\varepsilon - \varepsilon_y/1-\nu^2) \quad . \tag{3}$$

At failure, when the extensional strain (ε) exceeds a critical fracture strain (ε_F), the apparent stress intensity (K) will equal the apparent fracture toughness (K_A). Thus, ignoring small terms in Eq. (3),

an expression for the fracture toughness ahead of a radius notch for strain-controlled fracture can be given as

$$K_A \approx \left(\frac{3}{2}\ \sigma_y\ E\ \varepsilon_F\right)^{1/2}\ \rho^{1/2}\ . \qquad (4a)$$

Below some critical notch root radius, $\rho \leq \rho_o$, the fracture toughness is observed to be independent of ρ[31,32] (Fig. 12), and hence following the procedure of Tetelman and co-workers,[27,28] it may be postulated that

$$K_{Ic} \approx \left(\frac{3}{2}\ \sigma_y\ E\ \varepsilon_F\right)^{1/2}\ \rho_o^{1/2}\ . \qquad (4b)$$

The parameter ρ_o, the "effective" or limiting root radius, can be considered in this instance as a measure of the characteristic distance or gage length over which the critical strain must be exceeded to cause failure, and is a measure of the minimum amount of material ahead of the notch tip in which the failure initiation mechanisms can operate (see also Ref. 33). This distance should be related to the salient microstructural feature controlling fracture, which, in the case of particle-induced ductile rupture (microvoid coalescence), is likely to be closely associated with the particle spacing or distribution.

Using Eq. (4a) to rationalize the data shown in Fig. 12, it is clear that since the yield strength of as-quenched 4340 is independent of austenitizing temperature (Fig. 4), the slope of the K_A vs. $\rho^{1/2}$ plot is now a function of the critical fracture strain (ε_F), which is

a measure of ductility. The observed decrease in slope with increasing austenitizing temperature shown in Fig. 12, and thus the reduction in V-notch toughness (ie. Charpy energy) when $\rho > \rho_o$, can be attributed to a decrease in ductility found with increasing austenitizing temperature. Examination of the variation in uniaxial tensile ductility (ε_f) as a function of austenitizing temperature for as-quenched (Fig. 13) and quenched and tempered (Fig. 14) 4340 clearly verifies this trend. In fact the reduction in area of as-quenched 4340 is reduced dramatically from 30 pct after quenching from 870°C to a mere 10 pct after quenching from 1200°C. In strict terms, though, the ε_F term in Eq. (4a) refers to ductility in the region ahead of a notch under plane strain conditions, ie. to the plane strain ductility (ε_f'). In order to measure this quantity, a series of plane strain tension specimens (Fig. 3) was loaded for as-quenched 4340 austenitized at temperatures between 870°C and 1200°C. The results are plotted in Fig. 15 in terms of the variation of true fracture strain with austenitizing temperature, where the uniaxial and plane strain ductility values are compared with predicted values, computed from radius notch data in Fig. 12 using Eq. (4a). It is apparent that while the measured (ε_f') and predicted (ε_F) plane strain ductilities are not the same, the values do exhibit the identical trend of decreasing fracture strain with increasing austenitizing temperature. It is thus concluded that the decrease in rounded-notch toughness (ie. impact and slow bend Charpy values) with increase in austenitizing temperature can be closely associated with a decrease in ductility (ie. true strain at fracture) for strain-controlled failure by ductile rupture.

To explain the increase in fracture toughness (ie. K_{Ic}, K_{Id}), it is necessary to consider the situation ahead of a sharp crack ($\rho < \rho_o$), where the local stress-strain fields are non-uniform, and to evoke a modified criterion for failure such that the critical fracture strain is exceeded over a critically stressed volume, instead of merely at a point. With this criterion, a critical value of strain, $\varepsilon = \varepsilon_F$, is everywhere reached or exceeded over a characteristic distance ahead of the crack tip. This is an analogous situation to the initiation of stress-controlled fracture ahead of a sharp crack where the fracture stress must be exceeded over a microstructurally-significant characteristic distance, such as some multiple of the grain size.[16] Since fracture initiation ahead of a sharp crack must involve a minimum amount of material which is characteristic of the scale of physical events involved, the initiation event for ductile rupture where the displacements produced by internal necking between particles are critical, would not be possible over distances smaller than the particle spacing.[34] By raising the austenitizing temperature in the present steel, the microstructure is significantly coarsened (Fig. 16) with respect to increased prior austenite grain size (Fig. 10), increased martensite packet diameter (Fig. 16) and increased particle spacing (Fig. 11). It is believed that this coarsening, and in particular, the increased particle spacing, is responsible for the increase in sharp-crack toughness with austenitizing temperature (for non-stress controlled fractures). In effect, the greater distances between void-initiating particles enlarges the characteristic distance

ahead of the crack tip over which the fracture strain must be exceeded, which is equivalent to an increase in the parameter ρ_o in Eq. (4b). This is borne out by the increase in size and spacing of dimples which is observed on fracture surfaces as the austenitizing temperature is raised (Fig. 11), and is consistant with the increased dissolution of carbide particles[35,13] and sulfide inclusions[36,5] associated with high temperature austenitization.

Thus, summarizing, it has been shown that by increasing the austenitizing temperature for 4340 steel in both as-quenched and quenched and tempered conditions, the apparent paradox in toughness evaluation, increasing K_{Ic} and K_{Id} values concurrent with decreasing Charpy V-notch energies, is observed when fracture occurs by ductile rupture as well as by cleavage and intergranular mechanisms. For failure by strain-controlled microvoid coalescence, the decrease in rounded-notch toughness (slow bend and impact Charpy V-notch energies) has been attributed is a decrease in ductility or critical fracture strain. The increase in sharp-crack toughness (K_{Ic} and K_{Id}), on the other hand, has been associated with an increase in the characteristic distance over which the fracture strain must be exceeded ahead of the crack tip, apparently brought about by dissolution of void-initiating particles at high temperatures.

DISCUSSION

It may be seen from this investigation, together with the previous studies,[10,14] that the decrepancy in toughness evaluation, as measured by K_{Ic} and Charpy V-notch tests in ultra-high strength steels austenitized at increasing temperatures, can be attributed to a differing response of each microstructure to the notch root radius. This decrepancy is independent of the mechanisms of failure. For stress-controlled fracture (ie. intergranular and quasi-cleavage) the *decrease* in Charpy V-notch energy with increasing austenitizing temperature was associated with a reduction in critical fracture stress, whereas the *increase* in K_{Ic} was attributed to an increase in characteristic distance, through a coarsening of the microstructure (tentatively associated with increased prior austenite grain size).[10] In the present work, for failure by strain-controlled fracture (ie. ductile rupture), a similar explanation is invoked. The observed *decrease* in Charpy V-notch energy with increasing austenitizing temperature is related to a marked reduction in critical fracture strain, consistent with an observed decrease in uniaxial and plane strain ductility. Examination of the literature reveals that this reduction in ductility is observed, almost without exception, for low alloy steels austenitized at increasing temperatures,[4,6,10,13,14,18,35] and can be attributed to greater strain concentrations developed at the boundaries between the larger martensite packets. The corresponding *increase* in K_{Ic} again is associated with an increase in characteristic distance, which for

ductile rupture is interpreted in terms of an increase in particle spacing resulting from dissolution of carbides, and possibly sulfide inclusions, at higher solution temperatures.

A widely quoted explanation[1,4,6,19-21] for the increase in K_{Ic} at higher austenitizing temperatures (the corresponding decrease in Charpy energy was not considered) has been formulated on the presumption, from qualitative transmission electron microscopy studies, that larger proportions of austenite films* are retained around martensite plates and packets of laths (eg. Fig. 17) after austenitizing at high temperatures (ie. 1100-1200°C) compared to conventional heat-treatment at 870°C. This explanation was based on data for *as-quenched* (untempered) 4340[6] and Fe/C/Cr[21] steels. To investigate this quantitatively, tensile tests were performed on a series of untempered 4340, direct oil quenched from 870, 1000, 1100 and 1200°C, in which the percentage of retained austenite transformed with strain was monitored *in situ* using a magnetic saturation technique during the test. The results are shown in Fig. 18, where levels of retained austenite for each aus-enitizing temperature are plotted, both initially (ie. before loading) and at yield (ie. at 0.2 pct strain). From these results, it is clear that not only is there no difference in the amounts of retained austenite after different austenitizing treatments, but also the austenite is so mechanically unstable in the as-quenched

*Such films are typically 100 to 200 Å thick in oil-quenched 4340 type steels.[6]

structure than less than 1.5 pct remains untransformed at yield. Such "stress-assisted" transformation of retained austenite, which is very characteristic in 4340 type steels in as-quenched, untempered conditions, has been closely associated with a marked *degredation* in toughness in both 4340 and 300-M steels,[37] where mechanically unstable austenite is rapidly transformed to a brittle, high carbon, untempered martensite under elastic loading. It is thus unlikely that the presence of retained austenite films in as-quenched structures can provide for increased fracture resistance. In addition the amount of austenite appears independent of austenitizing temperature. This evidence along with the fracture surface appearance tends to discount the role of retained austenite in any way accounting for the increase in K_{Ic} with high temperature austenitization.

While it is felt that the analyses presented here, and in the previous study,[10] provide useful rationalizations for the "increase in K_{Ic}/decrease in Charpy energy" paradox in as-quenched and lightly tempered ultra-high strength steels, behavior can be somewhat different for such steels tempered at higher temperatures. For example, studies on 4340[7] and En25[11] steels have shown by tempering above 250°C, the toughness of structures austenitized at high temperatures is inferior to those conventionally austenitized when assessed by *both* K_{Ic} *and* Charpy impact tests. However, the considerable coarser prior austenite grain size developed at high solution temperatures markedly increases the effect of any impurity-induced grain boundary embrittlement,[10] which may occur at temperatures around 250°C as

tempered martensite embrittlement and at higher temperatures (~400 - 600°C) as temper embrittlement. Wood[7] has observed a marked tempered martensite embrittlement trough in K_{Ic} values for 4340 austenitized at 1200°C which is very small when the steel is austenitized at 870°C. However, it is worth noting that the significantly coarser structure and larger prior austenite grain size resulting from high temperature austenitization, while playing a somewhat suspect role with regard to improvements in toughness, has been associated with increased resistance to environmentally-assisted fracture in both sustained loading hydrogen-induced cracking[38] and in near-threshold (extremely low growth rate) fatigue crack propagation[39] tests. Thus, despite the apparent danger in utilizing such heat-treatment procedures for commercial application in low alloy steels, there may be certain specific advantages which still remain to be fully explored.

Finally, the results described in this paper, and those reported elsewhere,[4,6,9-15,18] highlight the total lack of direct correlation between K_{Ic} and Charpy V-notch impact toughness values in ultra-high strength steels. This is important to realize in view of the many empirical correlations[40-44] proposed relating K_{Ic} and Charpy data which are commonly used to predict fracture toughness values. These relationships pertain principally to lower strength steels[40,42,43] where they are useful for estimating K_{Ic} values which would otherwise be difficult and expensive to measure by standard techniques. However, none of these relationships can predict an inverse trend of increasing K_{Ic} with decreasing Charpy V-notch energy as has been observed in the

present steels. We therefore conclude, as in the previous study,[10] that evaluation of material toughness in ultra-high strength steels must include an assessment of resistance to fracture ahead of both sharp (ie. fatigue pre-cracked) and rounded (ie. V-notched) notches, if material processing parameters are drastically changed. For alloy design purposes, it appears insufficient to grade toughness solely in terms of K_{Ic} or Charpy V-notch energy alone; assessments of both sharp-crack K_{Ic} and rounded-notch Charpy impact energy are required.

CONCLUSIONS

From a study of the ambient temperature fracture behavior of commercial AISI 4340 ultra-high strength steel in a) as-quenched (untempered) and b) quenched and tempered at 200°C conditions, the following specific conclusions can be made:

i) Static and dynamic fracture toughness values (K_{Ic} and K_{Id} respectively) are observed to systematically *increase* as the austenitizing temperature is raised from 870 to 1100 or 1200°C (all structures being direct oil quenched); the yield strength remaining unchanged.

ii) Static (slow bend) and dynamic (impact) Charpy V-notch energies are observed to systematically *decrease* as the austenitizing temperature is raised from 870 to 1200°C.

iii) For failure by strain-controlled ductile rupture, the decrease in rounded-notch Charpy energy is associated with a reduction in critical fracture strain at increasing austenitizing temperatures, consistent with an observed decrease in uniaxial tensile and plane strain ductility.

iv) The increase in sharp-crack K_{Ic} values, for failure by ductile rupture, is associated with a larger "effective" root radius, or characteristic distance, for fracture, resulting from dissolution of void-initiating particles at high austenitizing temperatures.

v) The presence of films of retained austenite is considered to be unimportant in contributing to the variation in toughness arising from changes in austenitizing temperature.

vi) Existing empirical relationships between K_{Ic} and Charpy V-notch energy cannot predict the variation in toughness observed for the ultra-high strength steels investigated. Toughness evaluation in these steels must involve an assessment of both sharp-crack K_{Ic} and rounded-notch Charpy impact values.

ACKNOWLEDGEMENTS

The research was conducted under the auspices of the U.S. Energy Research and Development Administration through the Materials and Molecular Research Division of the Lawrence Berkeley Laboratory. The authors wish to thank Professors V. F. Zackay and E. R. Parker for helpful discussions, John R. Dillon for experimental assistance, and Dr. R. A. Wullaert, Mr. W. L. Server and Mr. J. W. Scheckard of Fracture Control Corporation in Goleta, CA for the use of instrumented Charpy impact testing facilities.

REFERENCES

1. E. R. Parker and V. F. Zackay: Eng. Fract. Mech., 1975, vol. 7, p. 371.
2. V. F. Zackay, E. R. Parker, R. D. Goolsby, and W. E. Wood: Nature Phys. Sci., 1972, vol. 236, p. 108.
3. G. Clark, R. O. Ritchie, and J. F. Knott: ibid, vol. 239, p. 104.
4. W. E. Wood, E. R. Parker, and V. F. Zackay: Rept. No. LBL-1474, Lawrence Berkeley Laboratory, University of California, Berkeley, Calif. 94720, May 1973.
5. R. O. Ritchie and J. F. Knott: Met. Trans., 1974, vol. 5, p. 782.
6. G. Y. Lai, W. E. Wood, R. A. Clark, V. F. Zackay, and E. R. Parker: ibid., p. 1663.
7. W. E. Wood: Eng. Fract. Mech., 1975, vol. 7, p.219.
8. J. L. Youngblood and M. R. Raghavan: Proc. AIAA/ASME/SAE 16th Structures, Structural Dynamics, and Materials Conf., Denver, Colorado, May 1975. (American Institute of Aeronautics and Astronautics, New York, N.Y.).
9. D. Dulieu: Discussion to paper by V. F. Zackay, E. R. Parker, and W. E. Wood; Proc. Third Intl. Conf. on the Strength of Metals and Alloys, vol. 2, p.383, Institute of Metals/Iron and Steel Institute, Cambridge, England, Aug. 1973.
10. R. O. Ritchie, B. Francis, and W. L. Server: Met. Trans. A, 1976, vol. 7A, p.831.
11. W. G. Ferguson, N. E. Clark, and B. R. Watson: Metals Technol., 1976, vol. 3, p.208.

12. S. Ensha and A. S. Tetelman: UCLA Tech. Rept. No. 14, UCLA-ENG-7435, School of Engineering and Applied Sciences, University of California, Los Angeles, Calif. 90024, May 1974.

13. M. F. Carlson, B. V. N. Rao, R. O. Ritchie, and G. Thomas: Proc. Fourth Intl. Conf. on the Strength of Metals and Alloys, vol. 2, p. 509, Nancy, France, Aug./Sept. 1976.

14. R. O. Ritchie, B. Francis, and W. L. Server: Met. Trans. A, 1977, vol. 8A, p.

15. S. Floreen: J. Eng. Mater. Tech., Trans. ASME Series H, 1977, vol. 99, p.70.

16. R. O. Ritchie, J. F. Knott, and J. R. Rice: J. Mech. Phys. Solids, 1973, vol. 21, p. 395.

17. W. E. Wood: Met. Trans. A, 1977, vol. 8A, p

18. E. H. Niccolls and P. A. Thornton: ibid, p

19. G. Thomas: Iron and Steel International, 1973, vol. 46, p. 451.

20. G. Y. Lai: Mater. Sci. Eng., 1975, vol. 19, p. 153.

21. J. A. McMahon and G. Thomas: Proc. Third Intl. Conf. on the Strength of Metals and Alloys, vol. 1, p. 180, Institute of Metals/Iron and Steel Institute, Cambridge, England, Aug. 1973.

22. Annual Book of ASTM Standards (American Society for Testing and Materials), ASTM Standards E399-74, Philadelphia, 1974.

23. Annual Book of ASTM Standards (American Society for Testing and Materials), p. 276, ASTM Standards E23-72, Philadelphia, 1972.

24. D. P. Clausing: Int. J. Fract. Mech., 1970, vol. 6, p. 71.

25. D. Bhandarkar, V. F. Zackay, and E. R. Parker: Met. Trans., 1972, vol. 3, p. 2619.

26. B. D. Cullity: in Elements of X-Ray Diffraction, p. 391, Addison-Wesley Publ. Co. Inc., 1959.

27. T. R. Wilshaw, C. A. Rau, and A. S. Tetelman: Eng. Fract. Mech., 1968, vol. 1, p. 191.

28. J. Malkin and A. S. Tetelman: ibid., 1971, vol. 3, p. 151.

29. P. T. Heald, G. M. Spink, and P. J. Worthington: Mater. Sci. Eng., 1972, vol. 10, p.129.

30. J. R. Rice: J. Applied Mechanics, Trans. ASME Series E , 1968, vol. 35, p. 379.

31. C. G. Chipperfield and J. F. Knott: Metals Technol., 1975, vol. 2, p. 45.

32. G. T. Hahn, R. G. Hoagland, and A. R. Rosenfield: Met. Trans. A, 1976, vol. 7A, p. 49.

33. A. C. MacKenzie, J. W. Hancock, and D. K. Brown: Eng. Fract. Mech., 1977, vol. 9, p. 167.

34. J. W. Hancock and A. C. MacKenzie: J. Mech. Phys. Solids, 1976, vol. 24, p. 147.

35. T. Tom: D. Eng. Thesis, Rept. No. LBL-1856, Lawrence Berkeley Laboratory, University of California, Berkeley, Calif. 94720, Sept. 1973.

36. B. J. Schulz and C. J. McMahon, Jr.: Met. Trans., 1973, vol. 4, p. 2485.

37. R. M. Horn and R. O. Ritchie: submitted to Met. Trans. A, 1977 (Lawrence Berkeley Laboratory Rept. No. LBL-6607, July 1977, University of California, Berkeley, Calif. 94720).

38. J. F. Lessar and W. W. Gerberich: Met. Trans. A, 1976, vol. 7A, p.953.

39. R. O. Ritchie: Metal Science, 1977, vol. 11, No. 8/9, p

40. J. M. Barsom and S. T. Rolfe: ASTM Spec. Tech. Publ. No. 466, p. 281, American Society for Testing and Materials, 1970.

41. J. G. Logan and B. Crossland: Proc. Conf. on Practical Appls. of Fract. Mech. to Pressure Vessel Tech., p. 148, Institute of Mechanical Engineers, London, 1971.

42. J. R. Hawthorne and T. R. Mager: ASTM Spec. Tech. Publ. No. 514, p. 151, American Society for Testing and Materials, 1972.

43. R. H. Sailors and H. T. Corten: ibid, p. 164.

44. P. N. Thorby and W. G. Ferguson: Mater. Sci. Eng., 1976, vol. 22, p. 177.

FIGURE CAPTIONS

Fig. 1. Model of the apparent paradox in toughness evaluation for *stress-controlled* fracture after Ritchie et al.[10] Shown is the distribution of tensile stress (σ_{yy}) at distance (r) ahead of stress concentrator at failure for a) structure direct quenched from 870°C (870°C structure) with sharp crack, b) structure step-quenched from 1200°C (1200-870°C structure) with sharp crack, c) 870°C structure with rounded notch (root radius ρ), and d) 1200-870°C structure with rounded notch. Critical fracture event occurs when $\sigma_{yy} > \sigma_F$ (the fracture stress) *over* characteristic distance (ℓ) ahead of sharp crack, or when $\sigma_{yy}^{max} \geq \sigma_F$ *at* the plastic-elastic interface ($r_c \gg \ell$) ahead of rounded notch. Toughness of 1200-870°C structure is greater ahead of sharp crack because characteristic distance is larger, toughness of 870°C structure is greater ahead of rounded notch because fracture stress (σ_F) is larger..

Fig. 2. Variation in prior austenite grain size with austenitizing temperature for direct oil quenched AISI 4340 steel.

Fig. 3. Design of plane strain tension specimen used to measure values of plane strain ductility.

Fig. 4. Variation of yield, ultimate tensile and true fracture stresses, measured in uniaxial tensile tests, with austenitizing temperature for as-quenched (untempered) AISI 4340 steel.

Fig. 5. Variation of yield, ultimate tensile and true fracture stresses with austenitizing temperature for AISI 4340 steel, direct oil quenched and tempered at 200°C.

Fig. 6. Variation of static and dynamic plane strain fracture toughness (K_{Ic} and K_{Id} respectively) of as-quenched (untempered) AISI 4340 steel with austenitizing temperature.

Fig. 7. Variation of static and dynamic Charpy V-notch energy, and area under tensile stress-strain curve, of as-quenched AISI 4340 with austenitizing temperature.

Fig. 8. Variation of plane strain fracture toughness (K_{Ic}) of 4340, quenched and tempered at 200°C, with austenitizing temperature.

Fig. 9. Variation of Charpy V-notch impact energy and area under tensile stress-strain curve of 4340 quenched and tempered at 200°C, with austenitizing temperature.

Fig. 10. Mechanisms of failure in as-quenched (untempered) 4340 steel, showing a) and b) ductile rupture and intergranular cracking in structure austenitized at 870°C, and c) and d) ductile rupture typical of structures austenitized at 1000, 1100 and 1200°C. All structures were direct oil quenched.

Fig. 11. Mechanisms of failure in 4340, quenched and tempered at 200°C showing ductile rupture (microvoid coalescence) in structures austenitized at a) 870°C, b) 1000°C, c) 1100°C and d) 1200°C. Note increased size and spacing of fracture dimples with increasing austenitizing temperature.

Fig. 12. Relationship between toughness, measured by the apparent fracture toughness (K_A) from slow-bend Charpy tests, and notch root radius (ρ) for as-quenched (untempered) 4340, austenitized at temperatures between 870 and 1200°C.

Fig. 13. Relationship showing the reduction in uniaxial tensile ductility with increasing austenitizing temperature for as-quenched 4340 steel.

Fig. 14. Relationship showing the reduction in uniaxial tensile ductility with increasing austenitizing temperature for 4340 steel, quenched and tempered at 200°C.

Fig. 15. Variation of true fracture strain with austenitizing temperature for as-quenched 4340 steel. Measured uniaxial and plane strain ductility values (ε_f and ε_f' respectively) are compared with predicted values (ε_F) computed from Eq. (4a) using data in Fig. 12.

Fig. 16. Optical micrographs of as-quenched martensitic structure in 4340, a) direct quenched from 870°C, and b) direct quenched from 1200°C, showing increased martensite packet size with increase in austenitizing temperature.

Fig. 17. Transmission electron micrographs of 4340, direct oil quenched from 1200°C, showing retained austenite films surrounding martensite laths: a) bright field image and b) dark field image of austenite reflextion showing reversal contrast of austenite films (after Lai et al.[6]).

Fig. 18. Variation of percentage of retained austenite, measured by magnetic saturation technique, with austenitizing temperature for as-quenched (untempered) 4340 steel. Plotted are initial (unstressed) levels and amounts un-transformed at yield (0.2 pct strain).

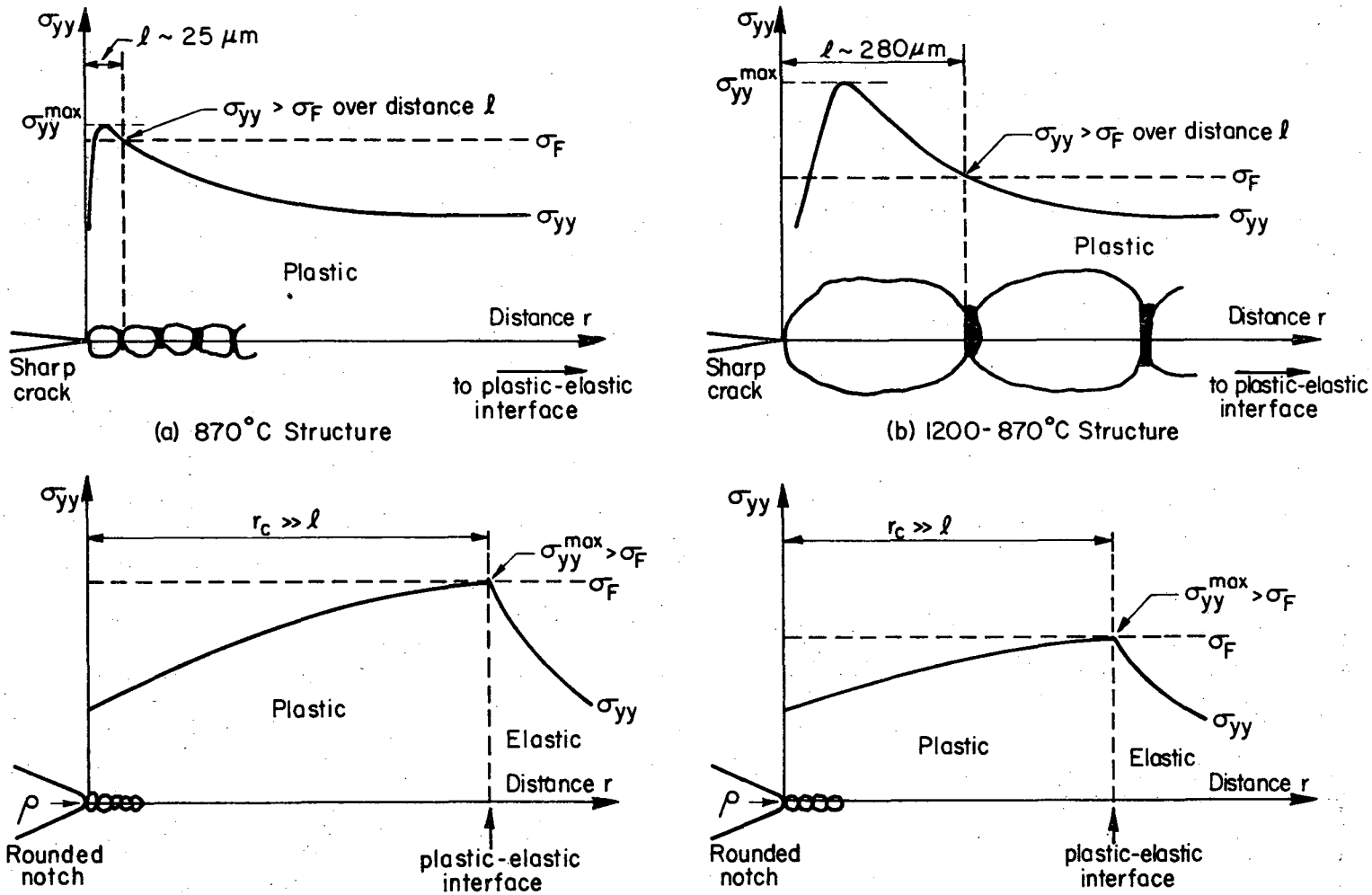

Fig. 1. Model of the apparent paradox in toughness evaluation for *stress-controlled* fracture after Ritchie et al.[10] Shown is the distribution of tensile stress (σ_{yy}) at distance (r) ahead of stress concentrator at failure for a) structure direct quenched from 870°C(870°C structure) with sharp crack, b) structure step-quenched from 1200-870°C structure) with sharp crack, c) 870°C structure with rounded notch (root radius ρ), and d) 1200-870°C structure with rounded notch. Critical fracture event occurs when $\sigma_{yy} > \sigma_F$ (the fracture stress) *over* characteristic distance (ℓ) ahead of sharp crack, or when $\sigma_{yy}^{max} \geq \sigma_F$ *at* the plastic-elastic interface ($r_c \gg \ell$) ahead of rounded notch. Toughness of 1200-870°C structure is greater ahead of sharp crack because characteristic distance is larger, toughness of 870°C structure is greater ahead of rounded notch because fracture stress (σ_F) is larger.

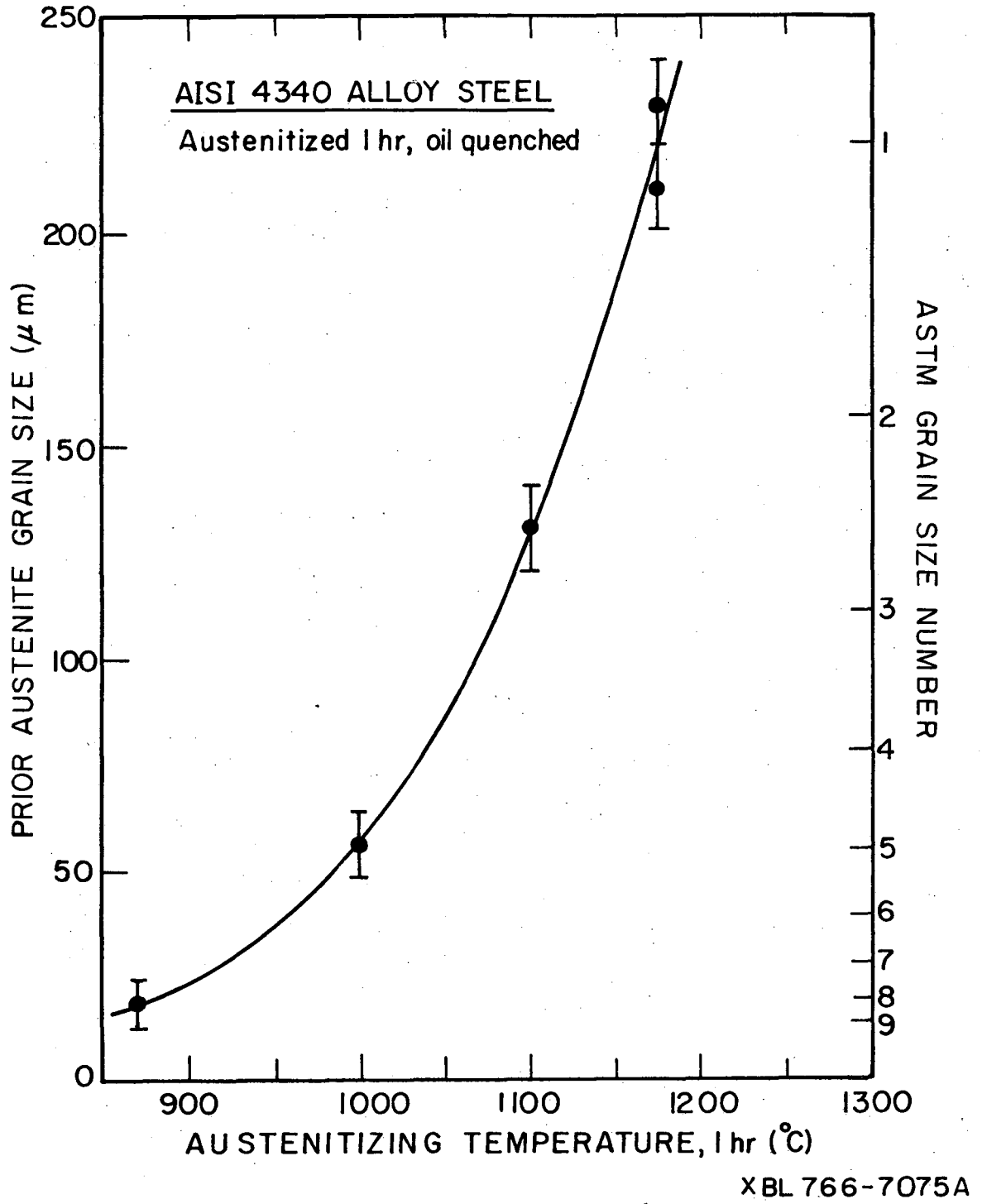

Fig. 2. Variation in prior austenite grain size with austenitizing temperature for direct oil quenched AISI 4340 steel.

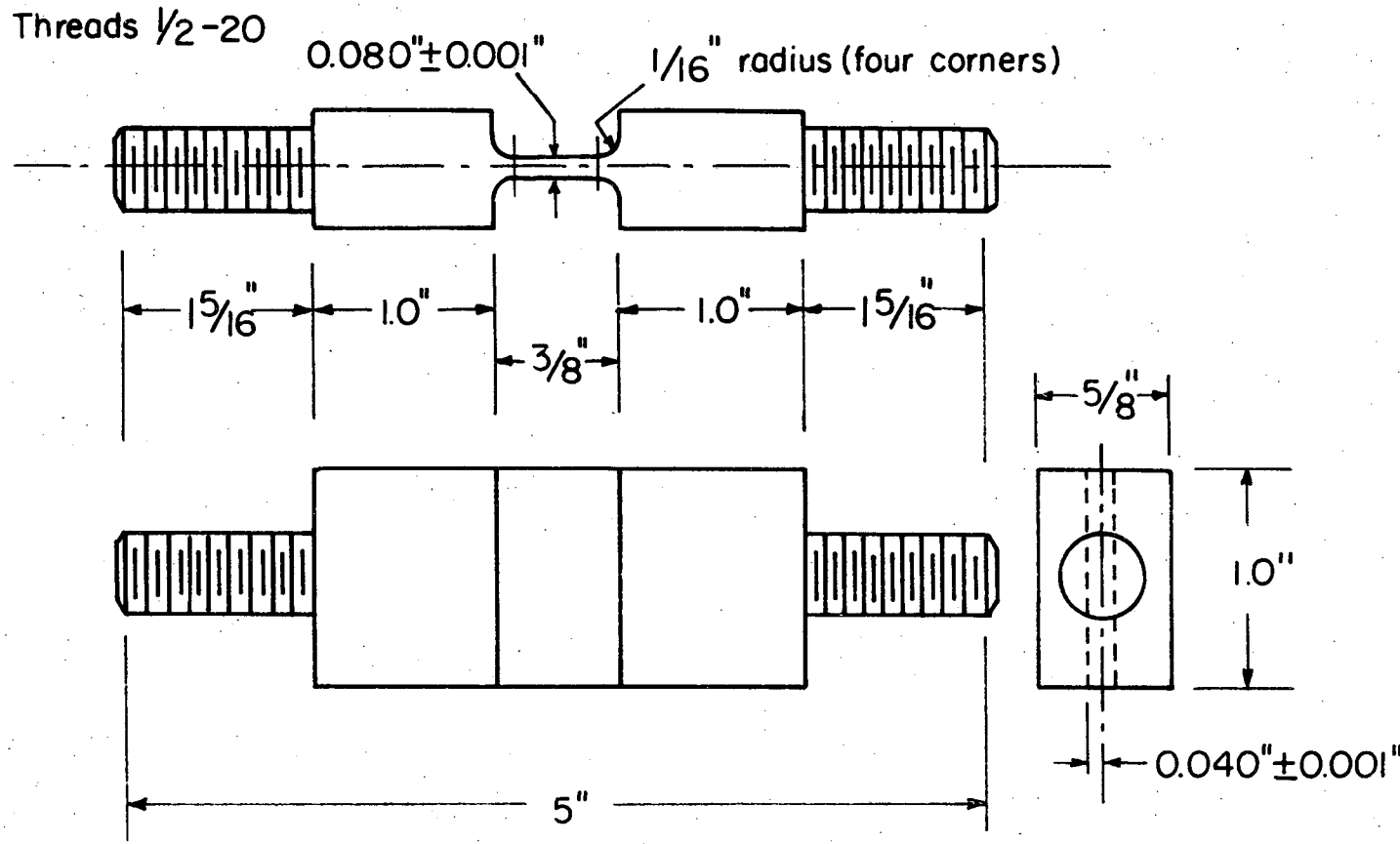

Fig. 3. Design of plane strain tension specimen used to measure values of plane strain ductility.

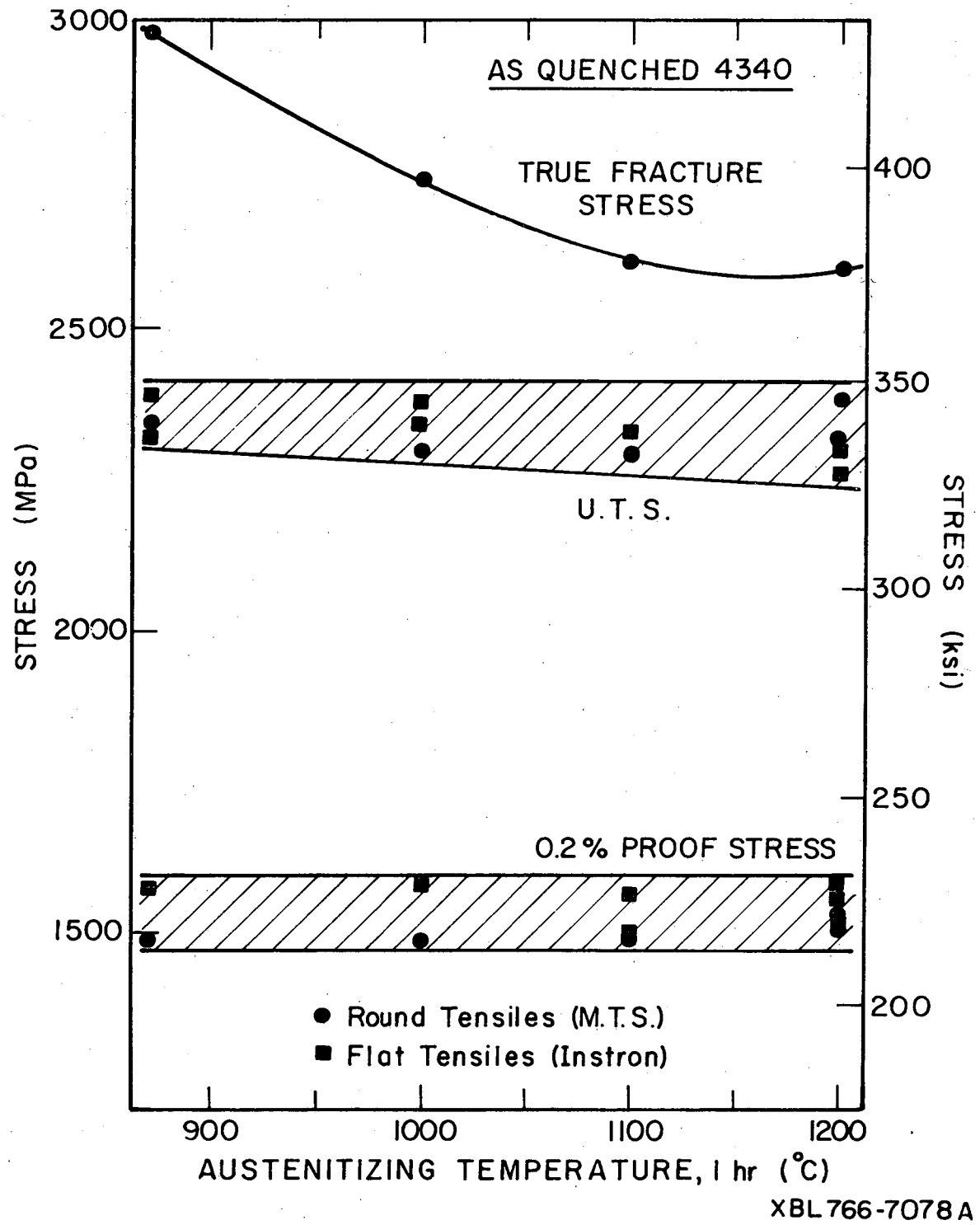

Fig. 4. Variation of yield, ultimate tensile and true fracture stresses, measured in uniaxial tensile tests, with austenitizing temperature for as-quenched (untempered) AISI 4340 steel.

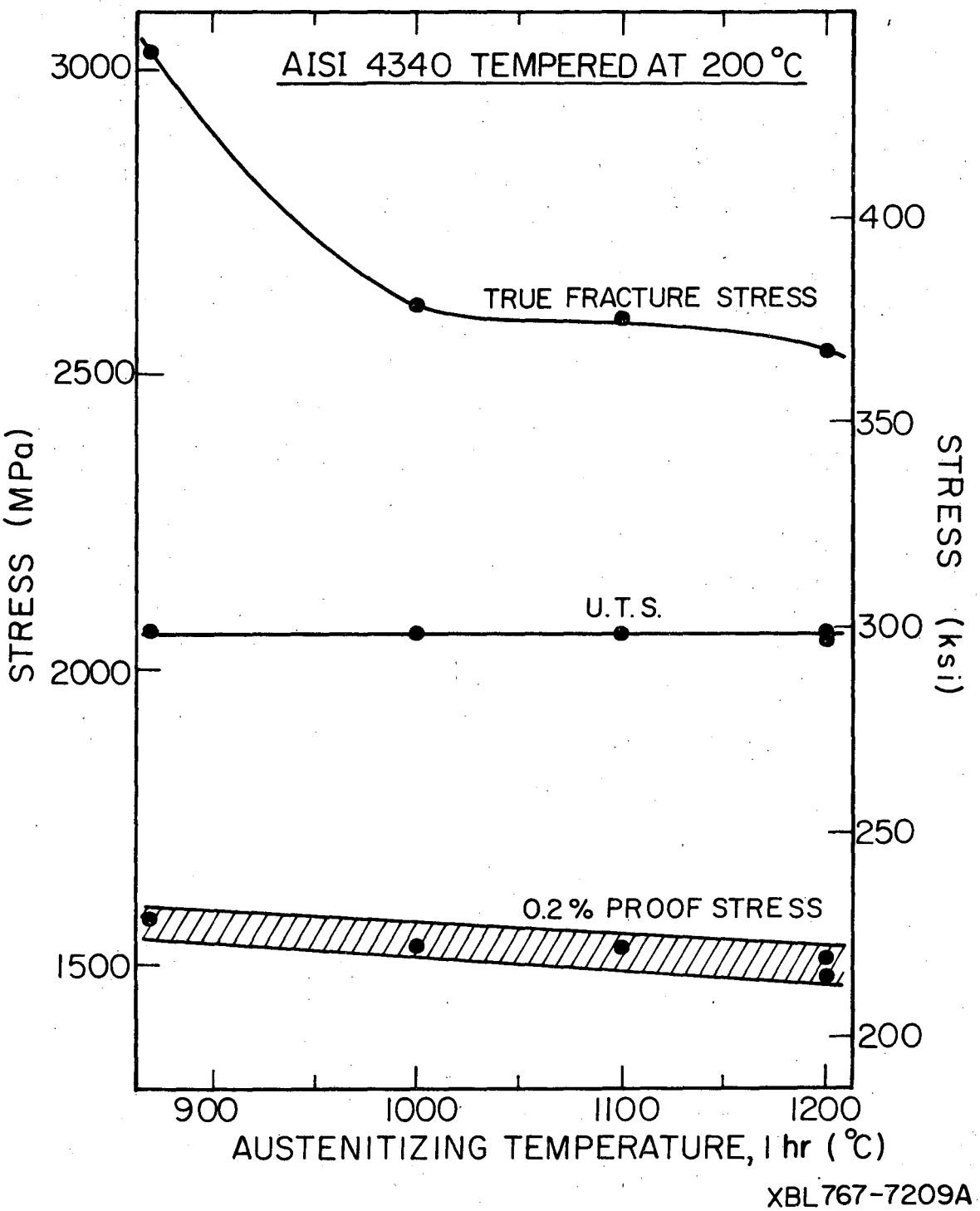

Fig. 5. Variation of yield, ultimate tensile and true fracture stresses with austenitizing temperature for AISI 4340 steel, direct oil quenched and tempered at 200°C.

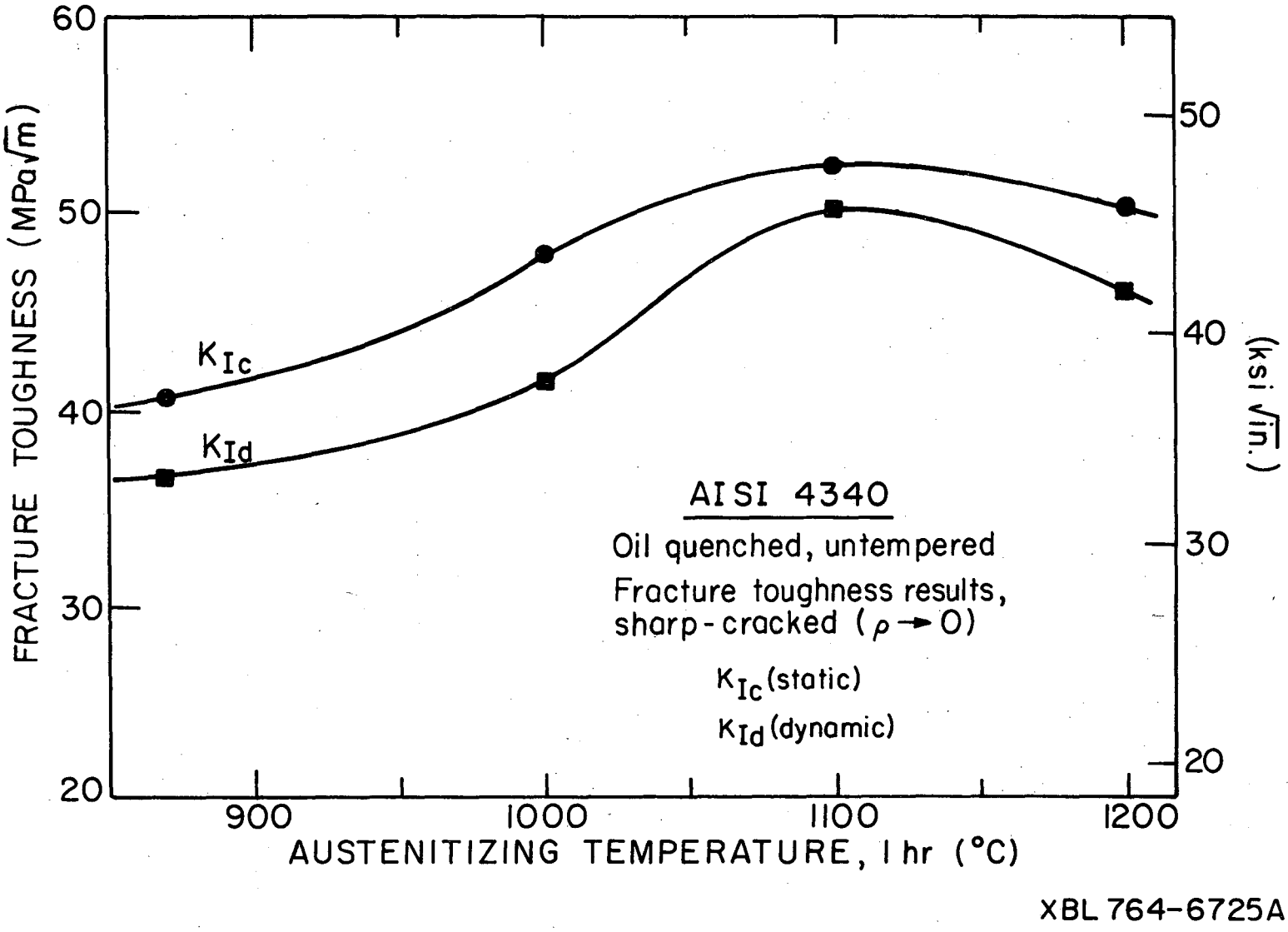

XBL 764-6725A

Fig. 6. Variation of static and dynamic plane strain fracture toughness (K_{Ic} and K_{Id} respectively) of as-quenched (untempered) AISI 4340 steel with austenitizing temperature.

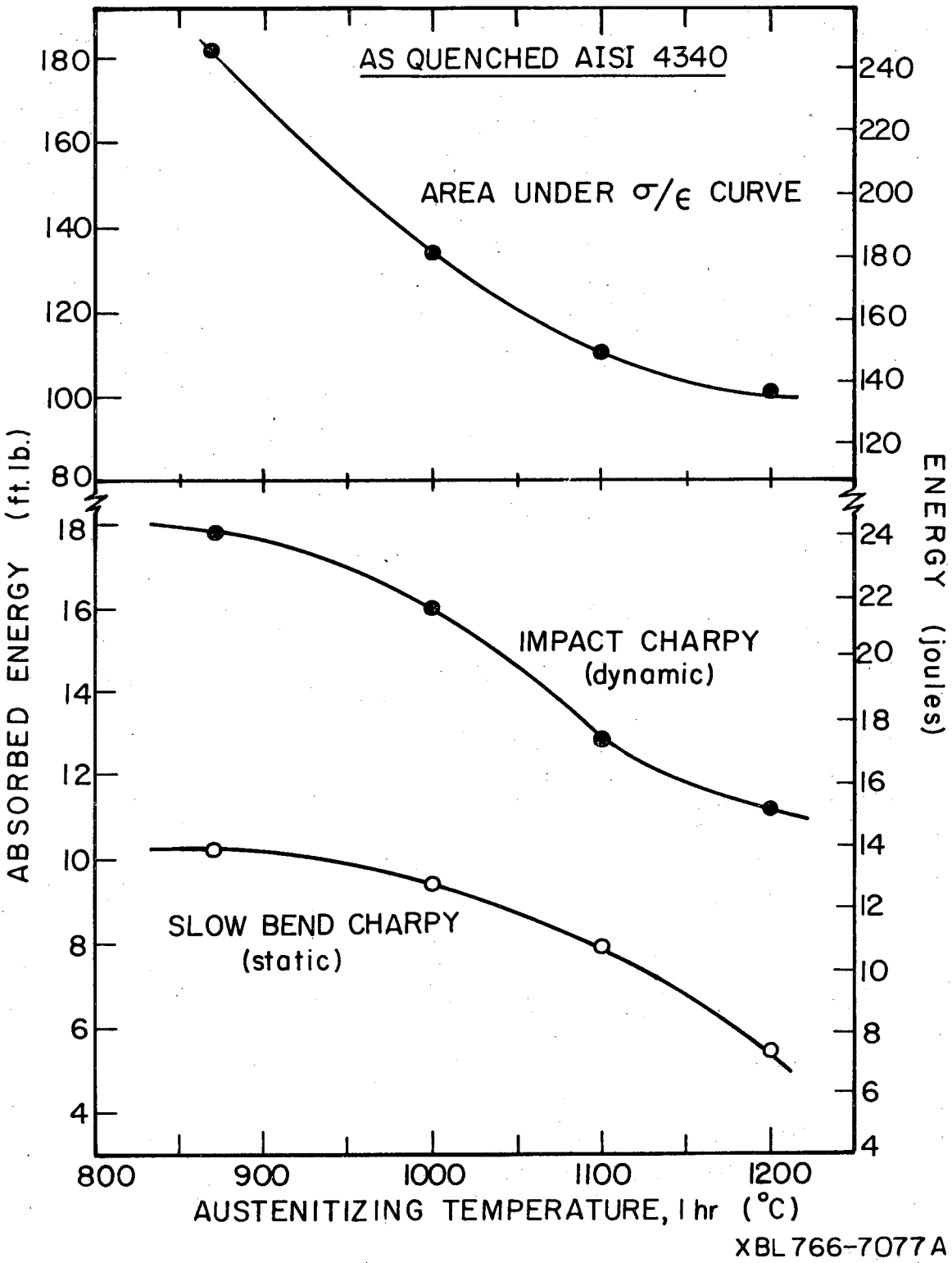

Fig. 7. Variation of static and dynamic Charpy V-notch energy, and area under tensile stress-strain curve, of as-quenched AISI 4340 with austenitizing temperature.

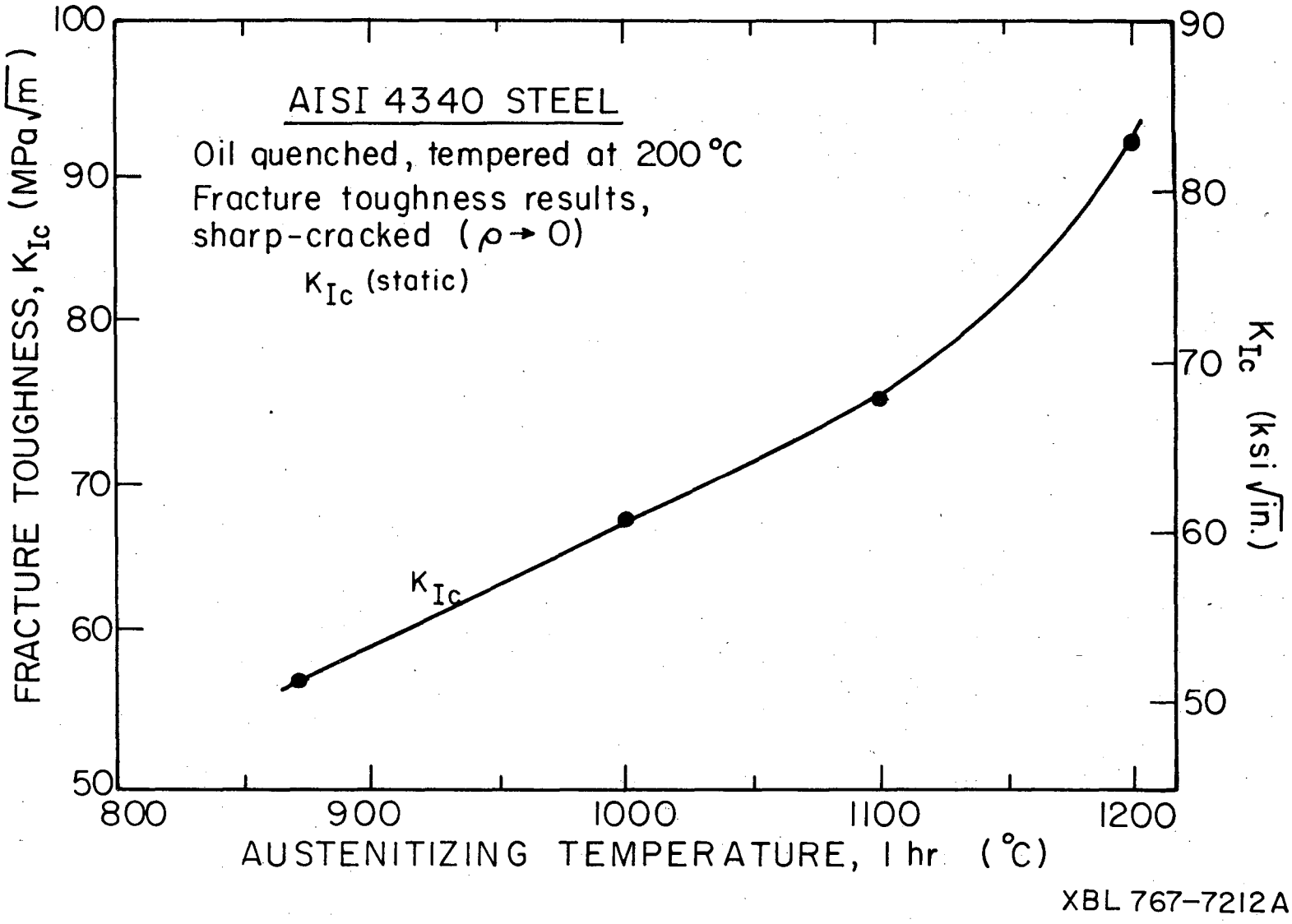

Fig. 8. Variation of plane strain fracture toughness (K_{Ic}) of 4340, quenched and tempered at 200°C, with austenitizing temperature.

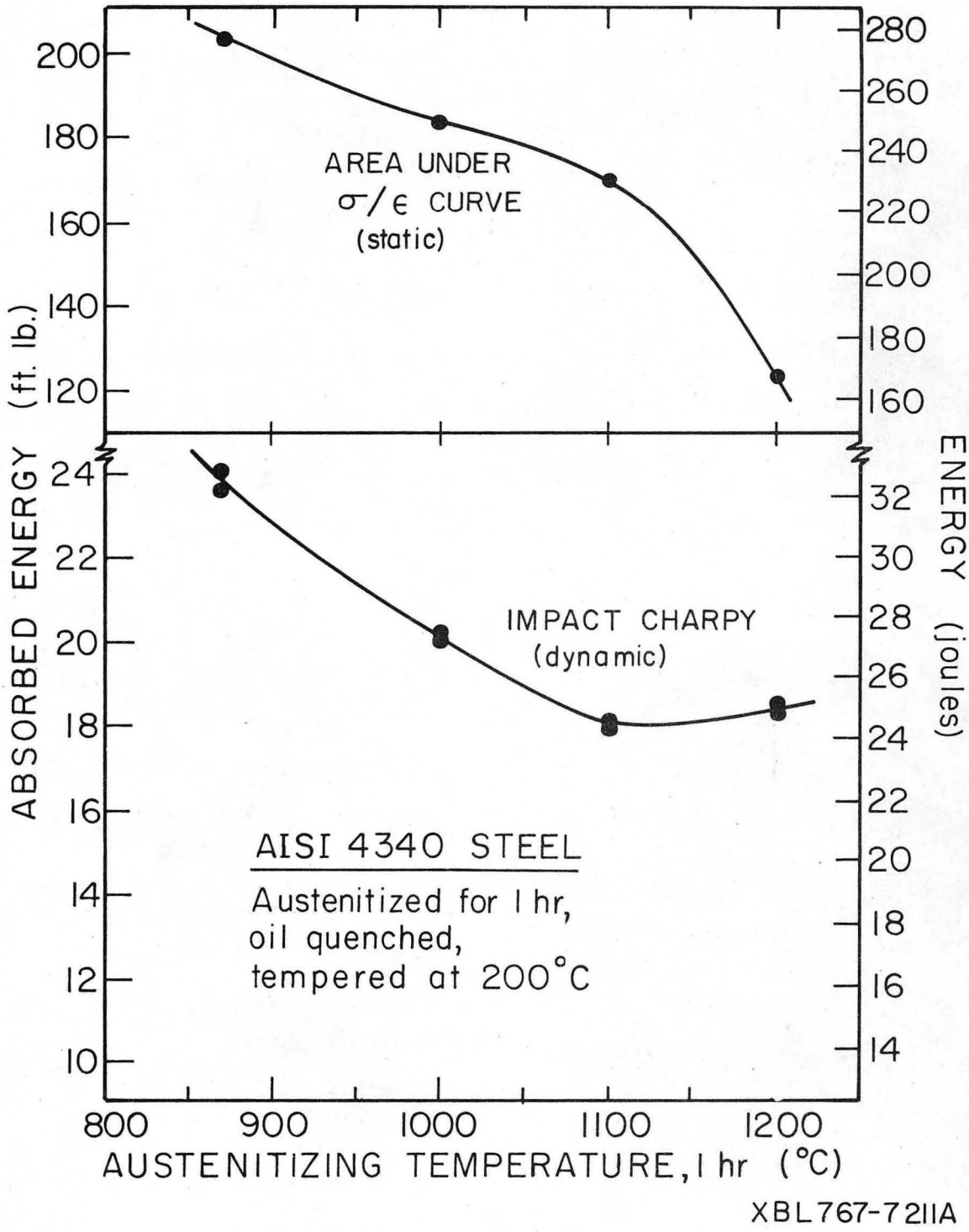

Fig. 9. Variation of Charpy V-notch impact energy and area under tensile stress-strain curve of 4340 quenched and tempered at 200°C, with austenitizing temperature.

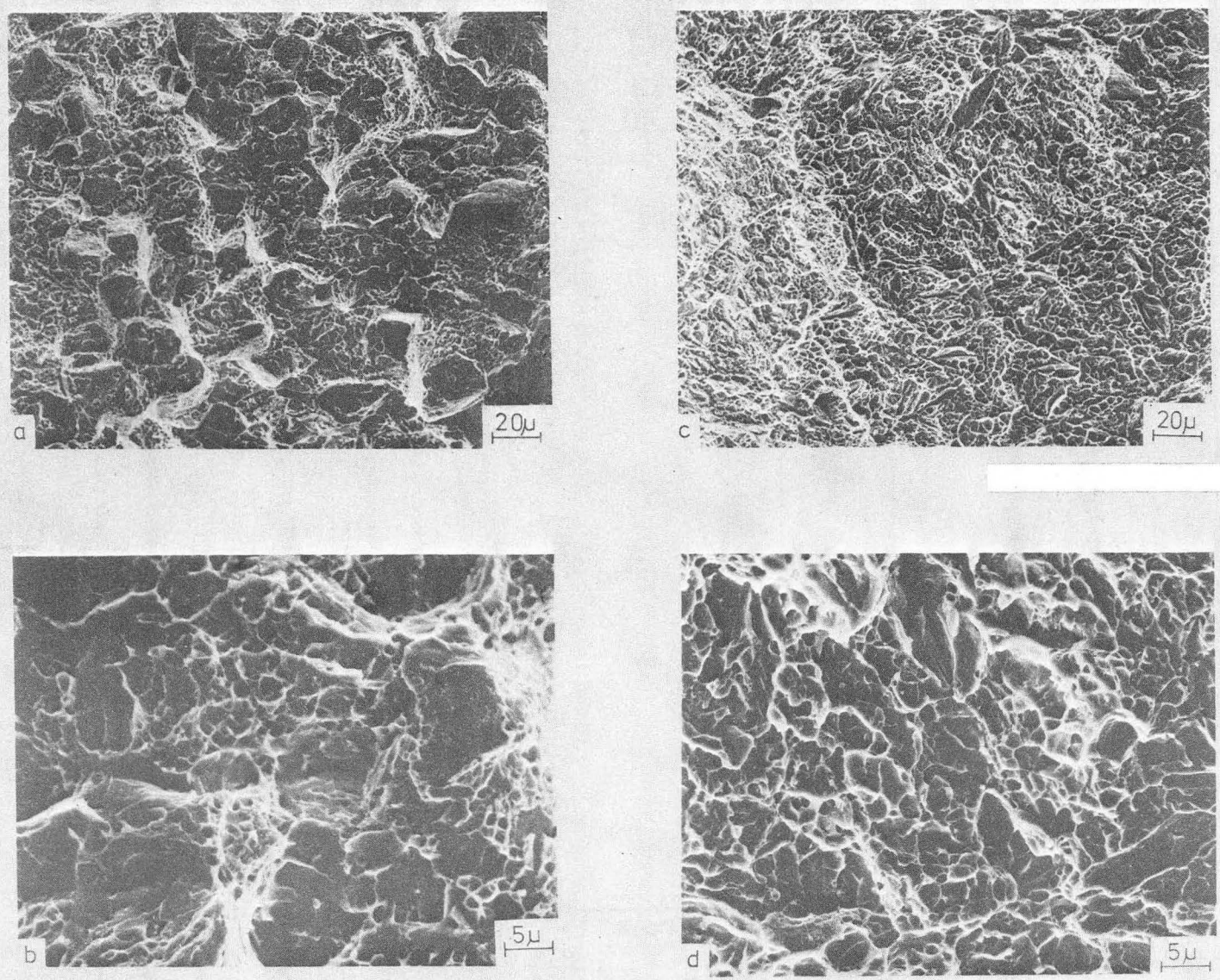

Fig. 10. Mechanisms of failure in as-quenched (untempered) 4340 steel, showing a) and b) ductile rupture and intergranular cracking in structure austenitized at 870°C, and c) and d) ductile rupture typical of structures austenitized at 1000, 1100 and 1200°C. All structures were direct oil quenched.

XBB 766-5545A

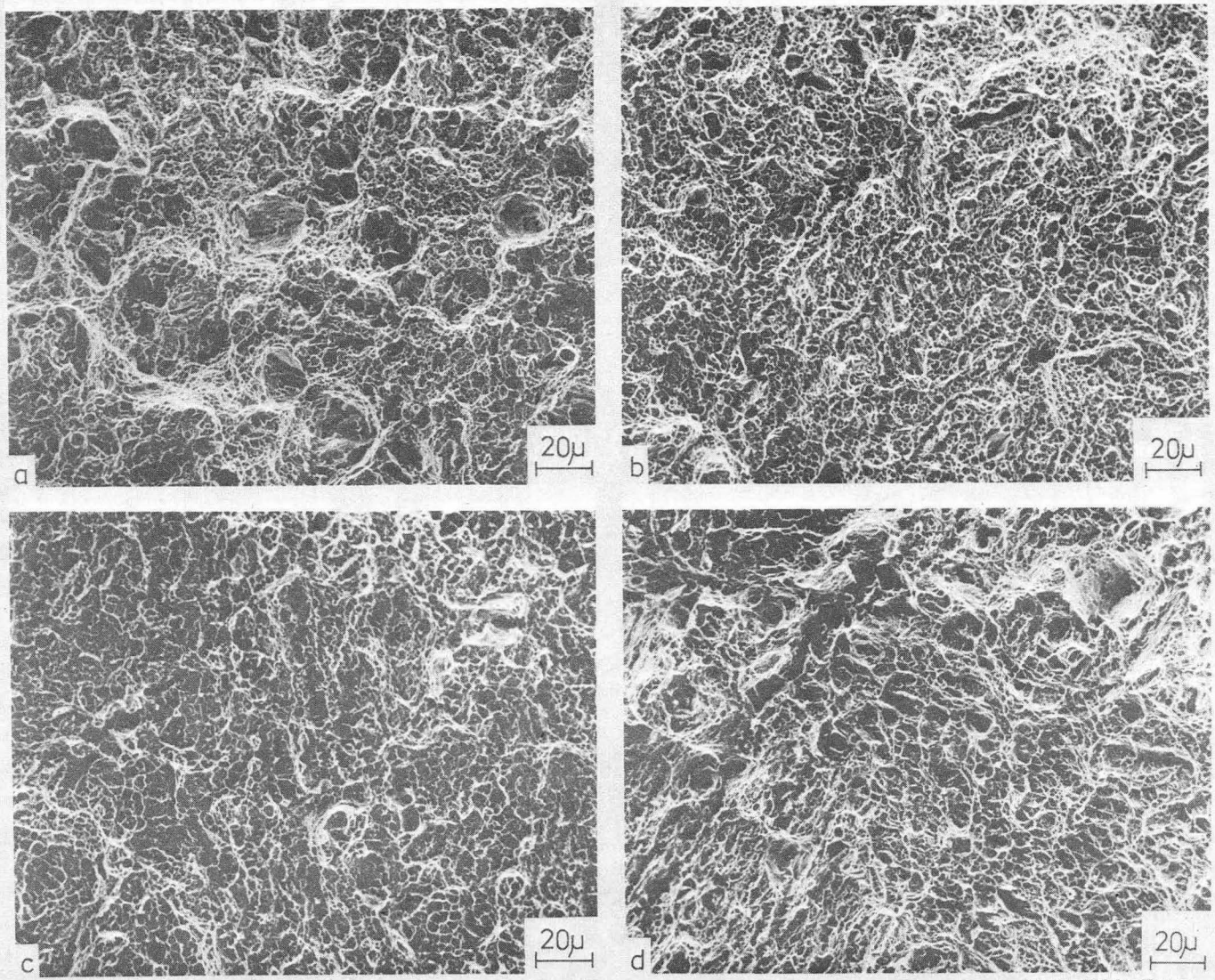

XBB 768-7121

Fig. 11. Mechanisms of failure in 4340, quenched and tempered at 200°C showing ductile rupture (microvoid coalescence) in structures austenitized at a) 870°C, b) 1000°C, c) 1100°C and d) 1200°C. Note increased size and spacing of fracture dimples with increasing austenitizing temperature.

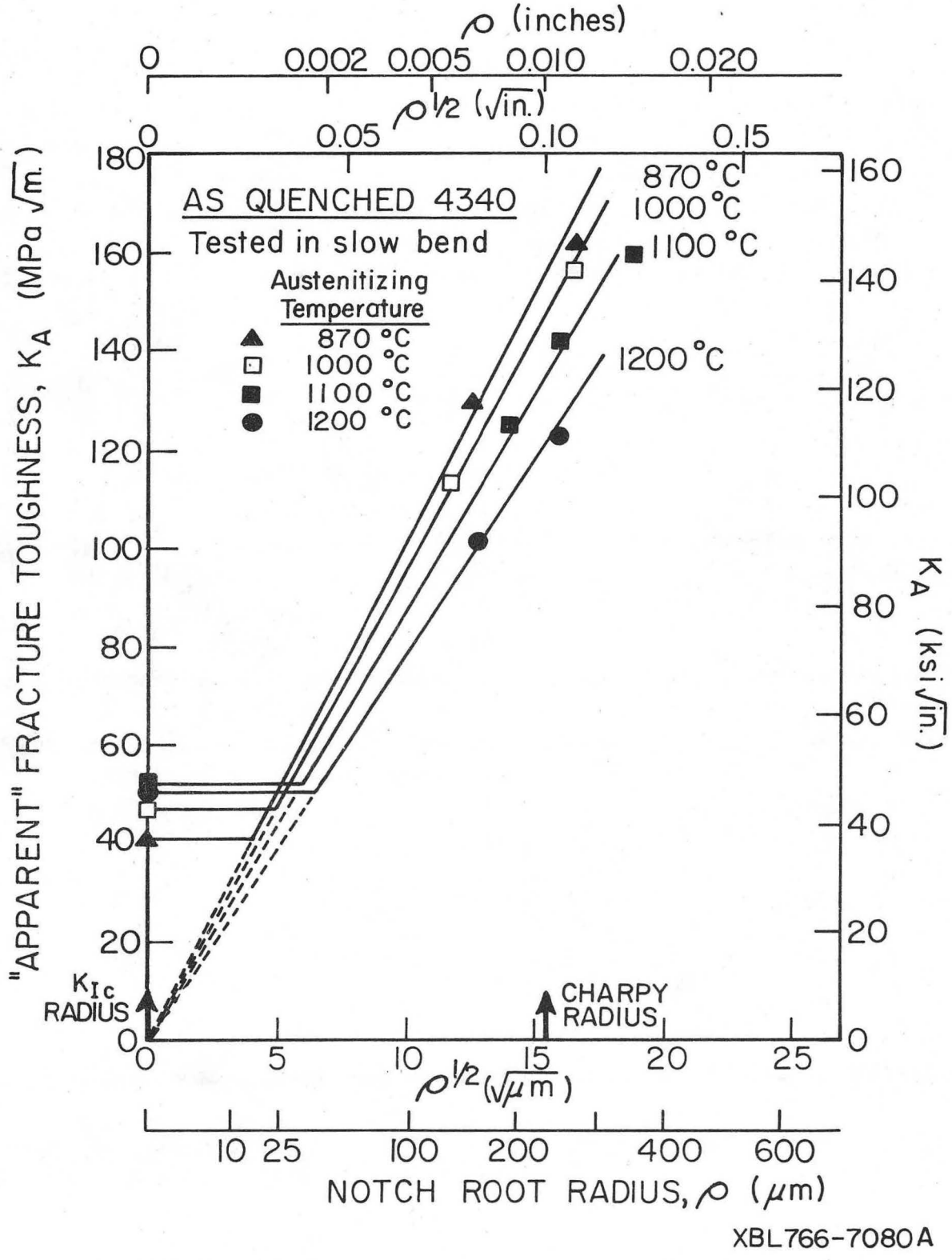

Fig. 12. Relationship between toughness, measured by the apparent fracture toughness (K_A) from slow-bend Charpy tests, and notch root radius (ρ) for as-quenched (untempered) 4340, austenitized at temperatures between 870 and 1200°C.

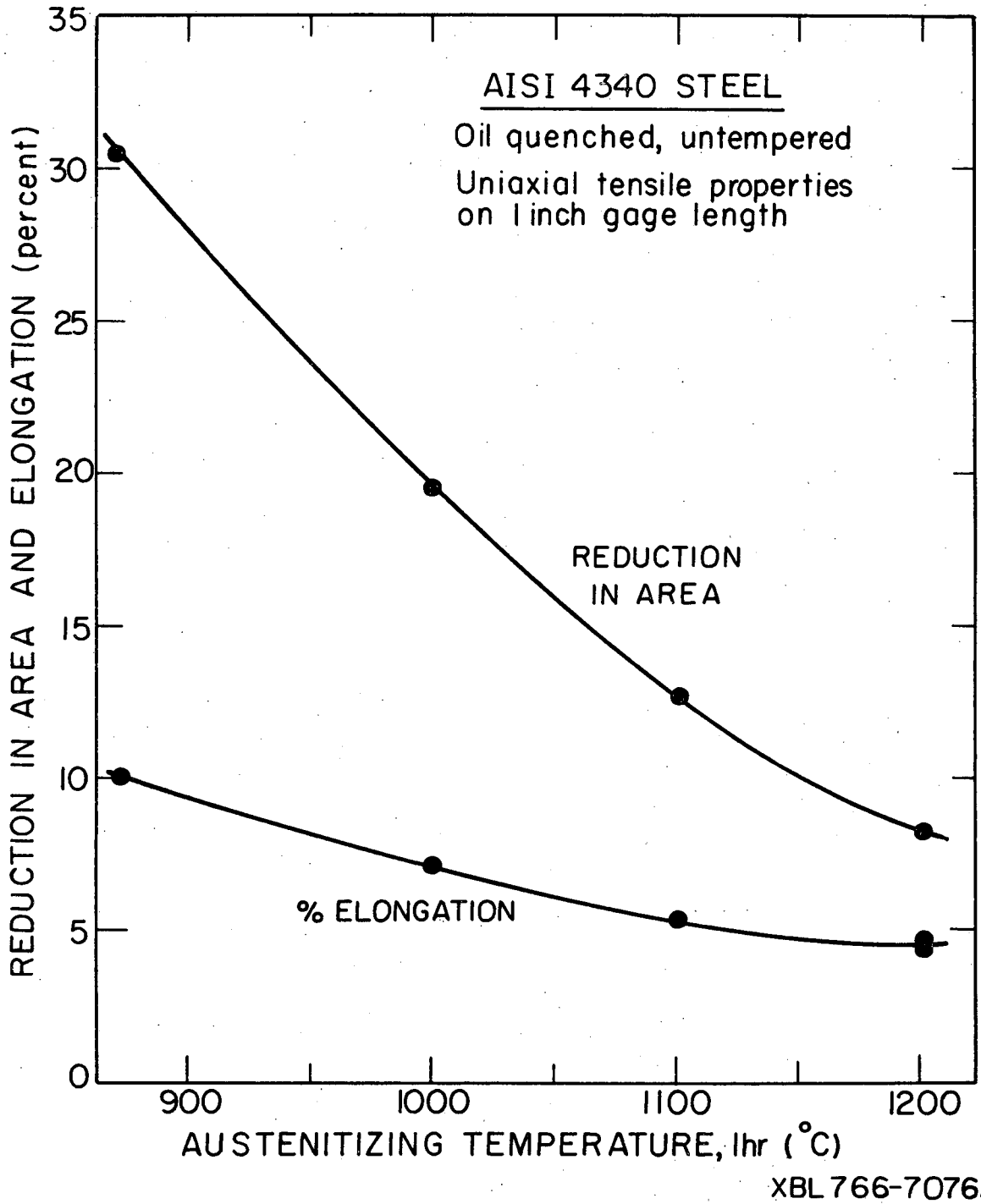

Fig. 13. Relationship showing the reduction in uniaxial tensile ductility with increasing austenitizing temperature for as-quenched 4340 steel.

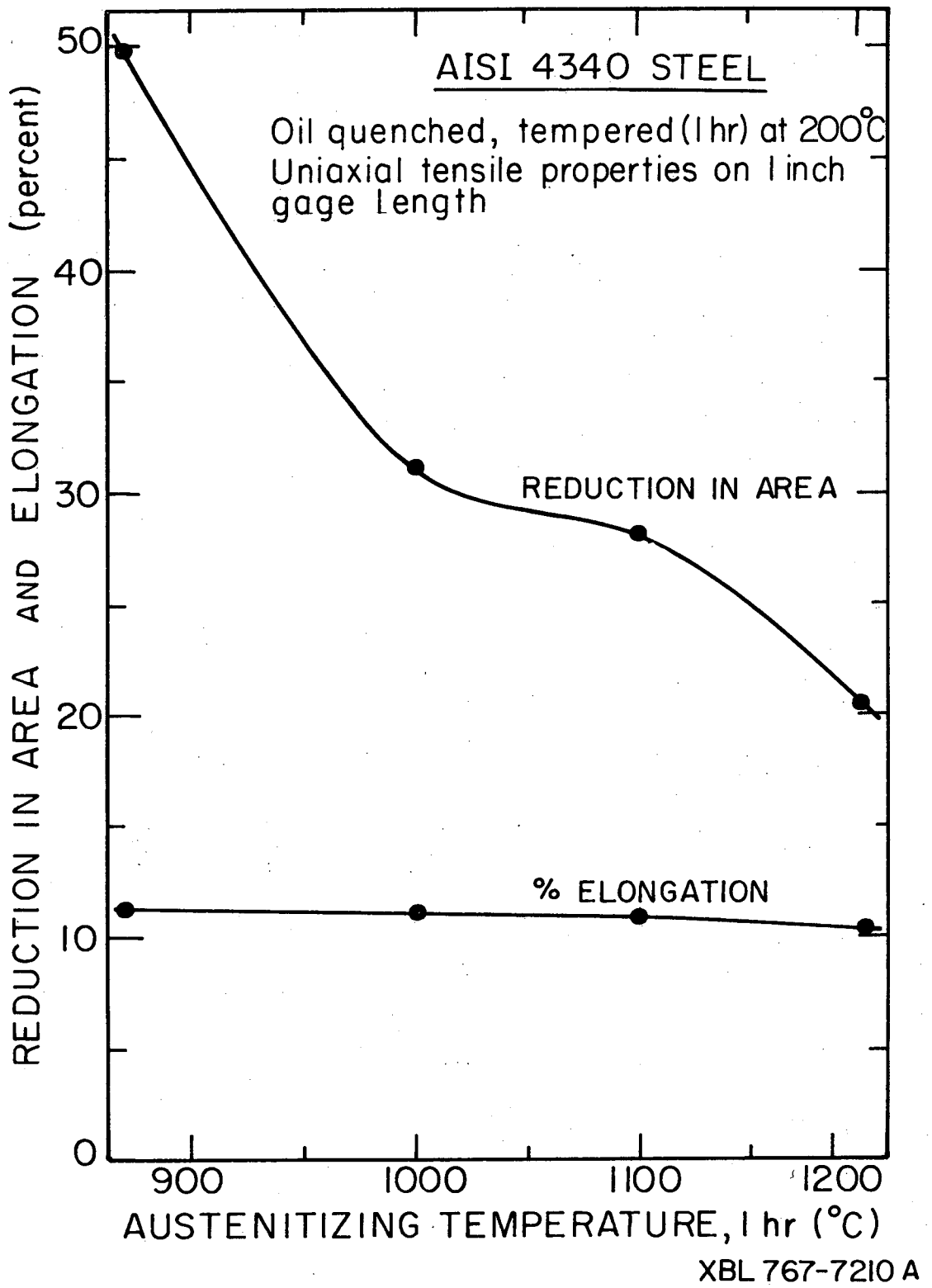

Fig. 14. Relationship showing the reduction in uniaxial tensile ductility with increasing austenitizing temperature for 4340 steel, quenched and tempered at 200°C.

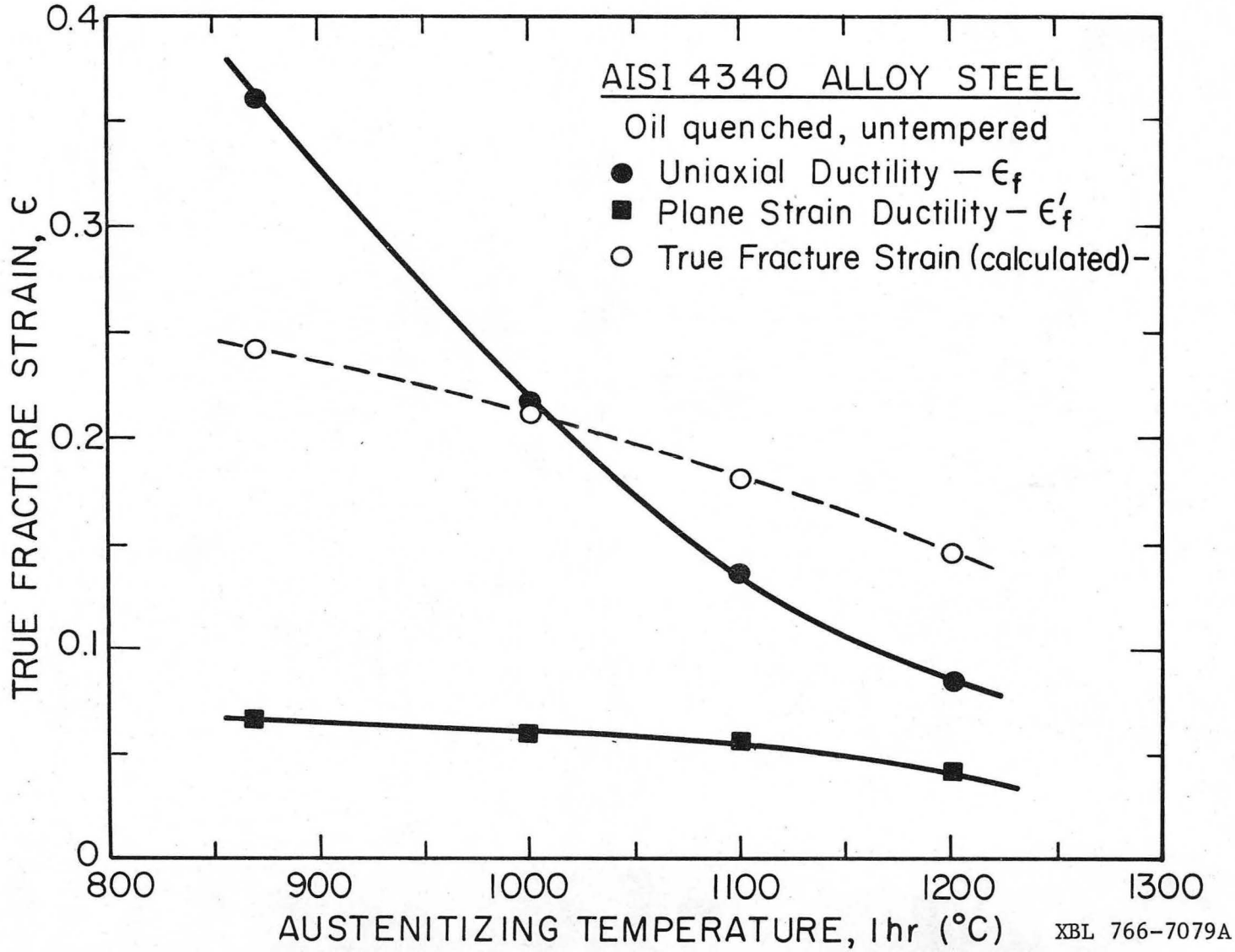

Fig. 15. Variation of true fracture strain with austenitizing temperature for as-quenched 4340 steel. Measured uniaxial and plane strain ductility values (ε_f and ε'_f respectively) are compared with predicted values (ε_F) computed from Eq. (4a) using data in Fig. 12.

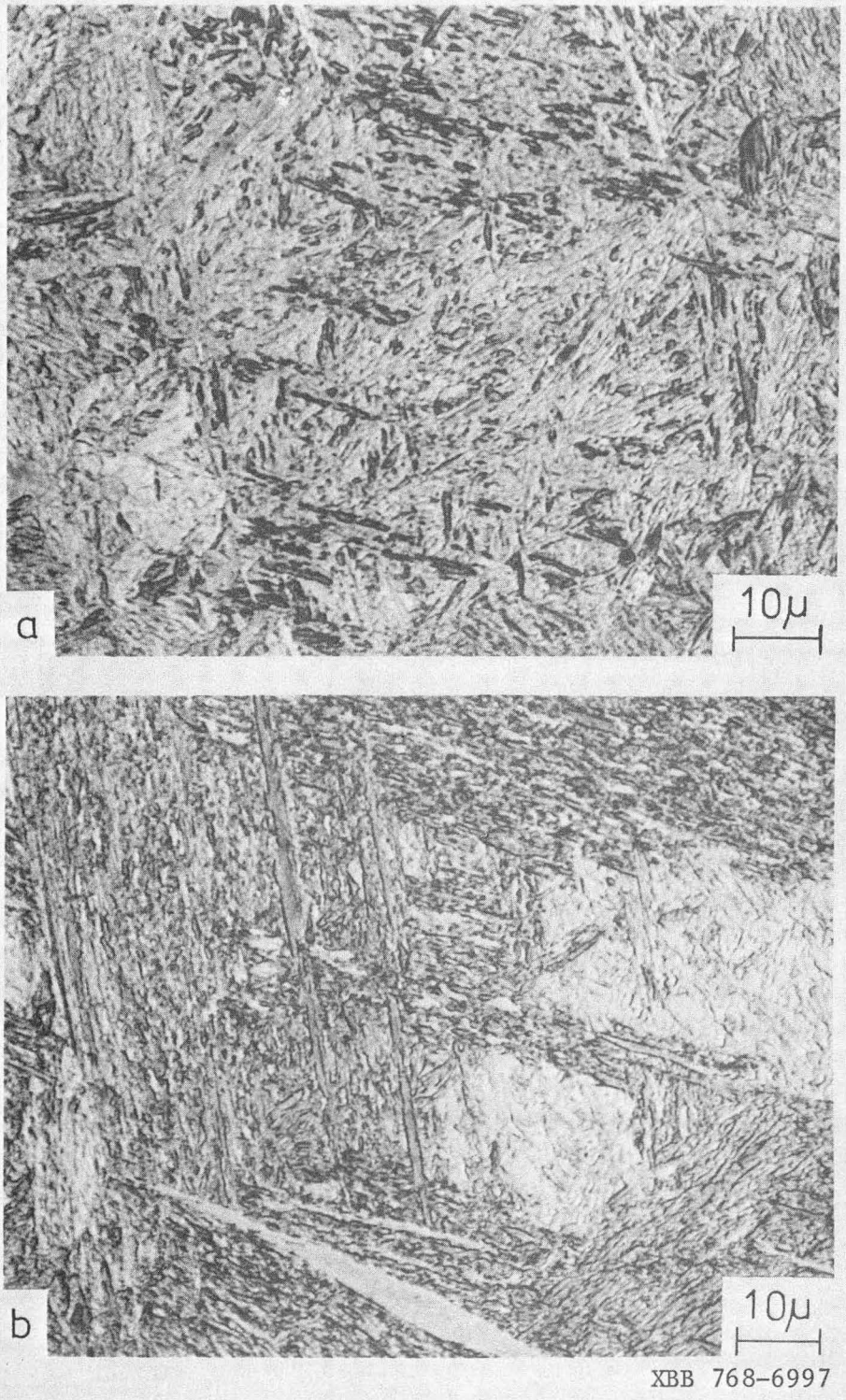

Fig. 16. Optical micrographs of as-quenched martensitic structure in 4340, a) direct quenched from 870°C, and b) direct quenched from 1200°C, showing increased martensite packet size with increase in austenitizing temperature.

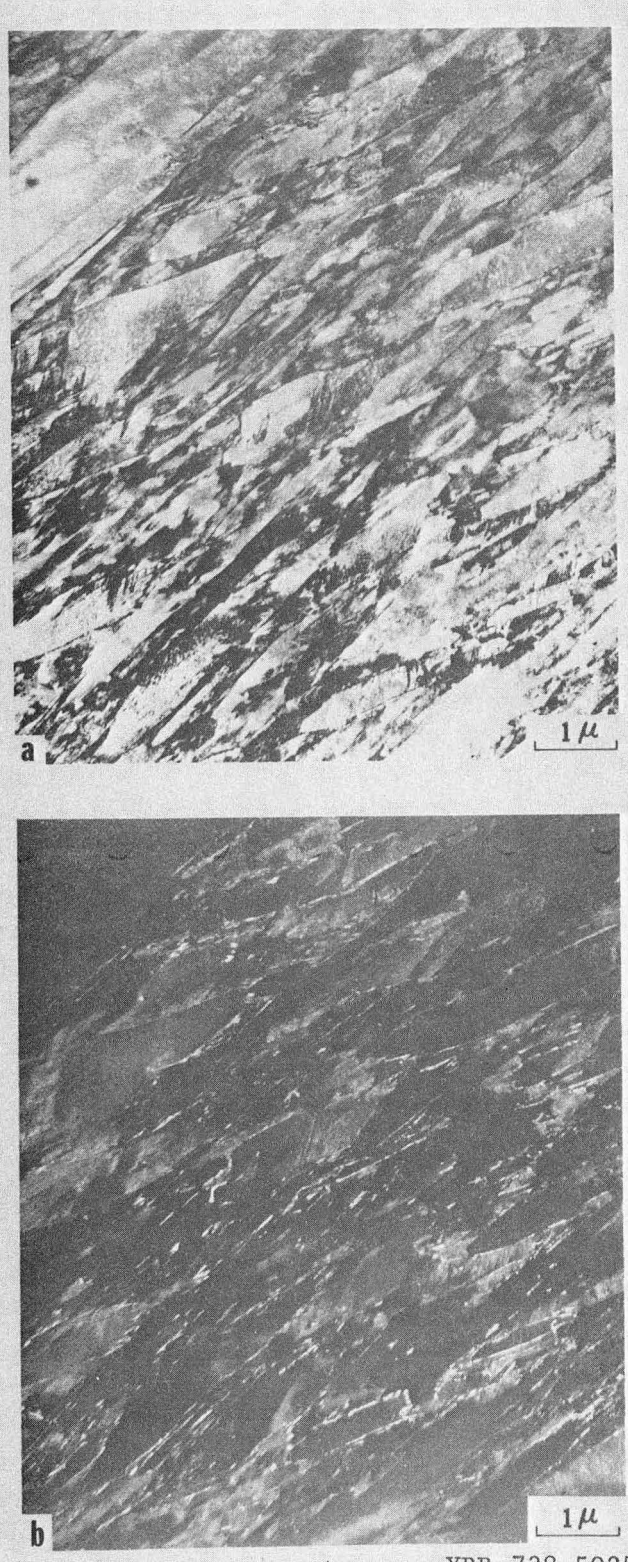

XBB 738-5025

Fig. 17. Transmission electron micrographs of 4340, direct oil quenched from 1200°C, showing retained austenite films surrounding martensite laths: a) bright field image and b) dark field image of austenite reflextion showing reversal contrast of austenite films (after Lai et al.[6]).

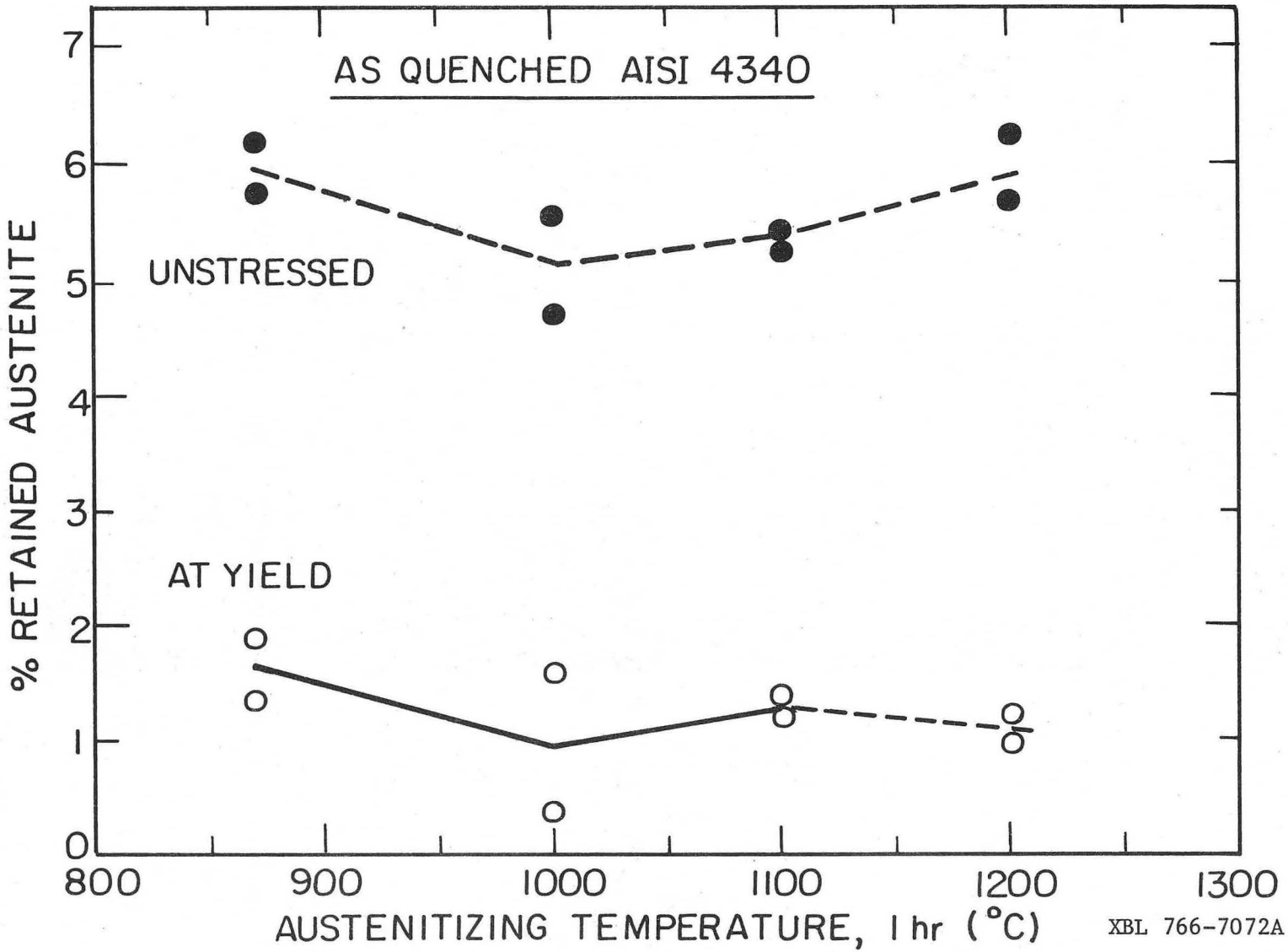

Fig. 18. Variation of percentage of retained austenite, measured by magnetic saturation technique, with austenitizing temperature for as-quenched (untempered) 4340 steel. Plotted are initial (unstressed) levels and amounts un-transformed at yield (0.2 pct strain).

TECHNICAL INFORMATION DEPARTMENT
LAWRENCE BERKELEY LABORATORY
UNIVERSITY OF CALIFORNIA
BERKELEY, CALIFORNIA 94720